NASA Contractor Report 179444

Spectral Contents Readout of Birefringent Sensor

Alex S. Redner

Contract NAS 2-12666
October 1989

National Aeronautics and
Space Administration

NASA Contractor Report 179444

Spectral Contents Readout of Birefringent Sensor

Alex S. Redner
Strainoptic Technologies, Inc., North Wales, PA

Prepared for
Ames Research Center
Dryden Flight Research Facility
Edwards, California
Under Contract NAS 2-12666

1989

National Aeronautics and
Space Administration
Ames Research Center
Dryden Flight Research Facility
Edwards, California 93523-5000

TABLE OF CONTENTS

1. SUMMARY

The objective of the research and development work carried on by STRAIN-OPTIC July 13, 1987 to July 12, 1989 was to develop a BIREFRINGENT SENSOR, capable of operation at room and elevated temperature, and a read-out method based on SPECTRAL CONTENTS ANALYSIS (SCA) method, for measurements of the stress/strain induced birefringence in the sensor. The feasibility study of this concept was demonstrated during the Phase I research.

As a result of the research, development and engineering efforts, the following results were accomplished:

a. Several candidate materials were investigated, and found suitable for use as a sensor at room temperature.

   For elevated temperature use, fused silica was found most satisfactory. This material was extensively evaluated and its BREWSTER CONSTANT calibrated up to 1000° C (2000° F).

b. The SPECTRAL CONTENTS ANALYSIS METHOD was fully developed and a working prototype was produced. Methods were developed to measure the birefringence and retardation in the range up to 6000 nm.

c. The data acquisition method developed incorporates:

   - Multipoint capability
   - Self-calibrate capability
   - Dynamic capability
   - Elevated temperature capability

d. Testing of the system was carried out to evaluated its capabilities. Birefringence was measured successfully at 2000° F.

All the research objectives were met, or exceeded. The Phase II research implementation of the method in commercial devices is now in progress.

2. INTRODUCTION

2.1. POLARIZED LIGHT - FUNDAMENTALS

Light propagates in transparent materials as an electromagnetic vibration. An incandescent source emits energy which propagates in all directions and contains a whole "spectrum" of vibrations of different frequencies or wavelengths.

Light propagates in a vacuum or in air at a speed (C) of 3×10^{10} cm/sec. In other transparent bodies, the speed V is lower and the ratio $n = C/V$ is called the index of refraction. In an isotropic body this index is constant, regardless of the direction of propagation or plane of vibration. However, in a stressed material the index depends upon the orientation of vibration with respect to its axis, and of the state of stress.

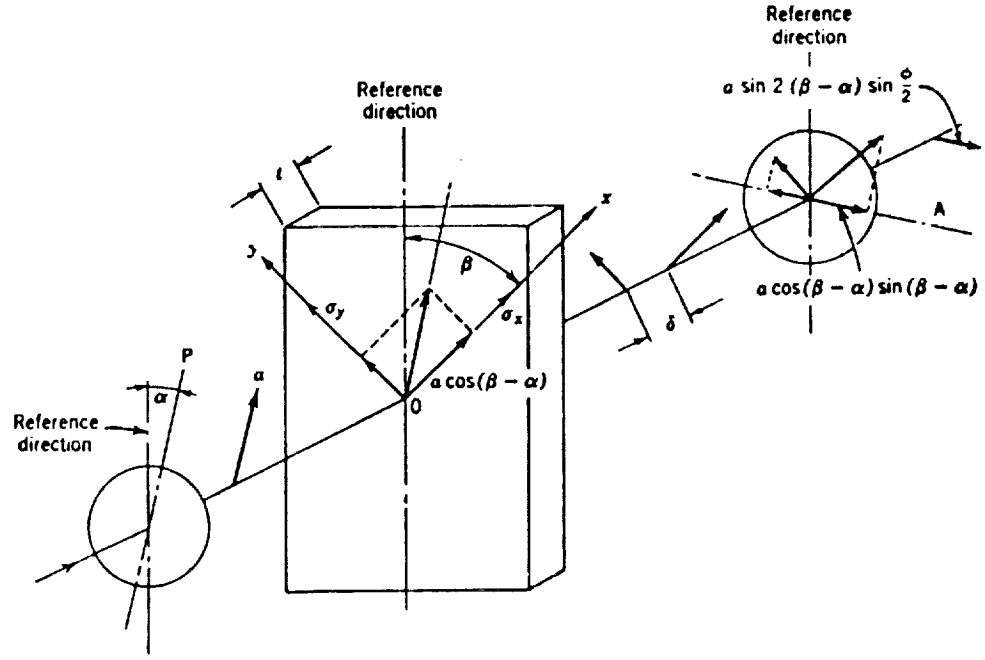

Fig. 1. Principle of a plane polariscope: P, plane of axis of polarizer; α, angle between polarizer and reference direction; a, amplitude of light polarized in plane P; t, thickness of sample containing stresses σ_x and σ_y in the x and y directions; β, angle between principal direction x and reference direction; δ, relative retardation of Y with respect to X wave; A, plane of axis of analyzer.

The change in index of refraction is a function of the stress applied. Brewster's Law established that the relative change in index of refraction is proportional to the difference of principal strains:

$$(n_x - n_y) = K\,(\varepsilon_x - \varepsilon_y)$$

or

$$(n_x - n_y) = C_B\,(\sigma_x - \sigma_y) \qquad (1)$$

The constant (K), is called the "strain-optical coefficient" and characterizes a physical property of the material, established by calibration. The constant C_B is the "stress-optical" Brewster's constant.

When a polarized beam (P) propagates through a transparent material of thickness t, where x and y are the directions of principal strains at the point under consideration, the light vector splits into two polarized beams vibrating in planes "x" and "y". (Figure 1)

If the strains along "x" and "y" are ε_x and ε_y and the speed of the light vibrating in these directions is V_x and V_y respectively, the time necessary to cross the plate for each of them will be t/V, and the relative retardation between these two beams is:

$$\delta = C\left(\frac{t}{V_x} - \frac{t}{V_y}\right) = t\,(n_x - n_y) \qquad (2)$$

Combining the expressions above we have:

$$\delta = tK\,(\varepsilon_x - \varepsilon_y) \qquad (3)$$

or, relating the retardation δ to stresses we have:

$$\delta = C_B t\,(\sigma_x - \sigma_y) \qquad (4)$$

Due to the relative retardation (distance between the fast and slow waves) δ, the two waves are no longer simultaneous when emerging from the specimen. The analyzer A will transmit only one component of each of these waves (that is parallel to A) as shown on Figure 2. These waves will interfere and the resulting light intensity will be a function of:

- -the retardation δ
- -the angle between the anlyzer and direction of principal stresses $(\beta - \alpha)$

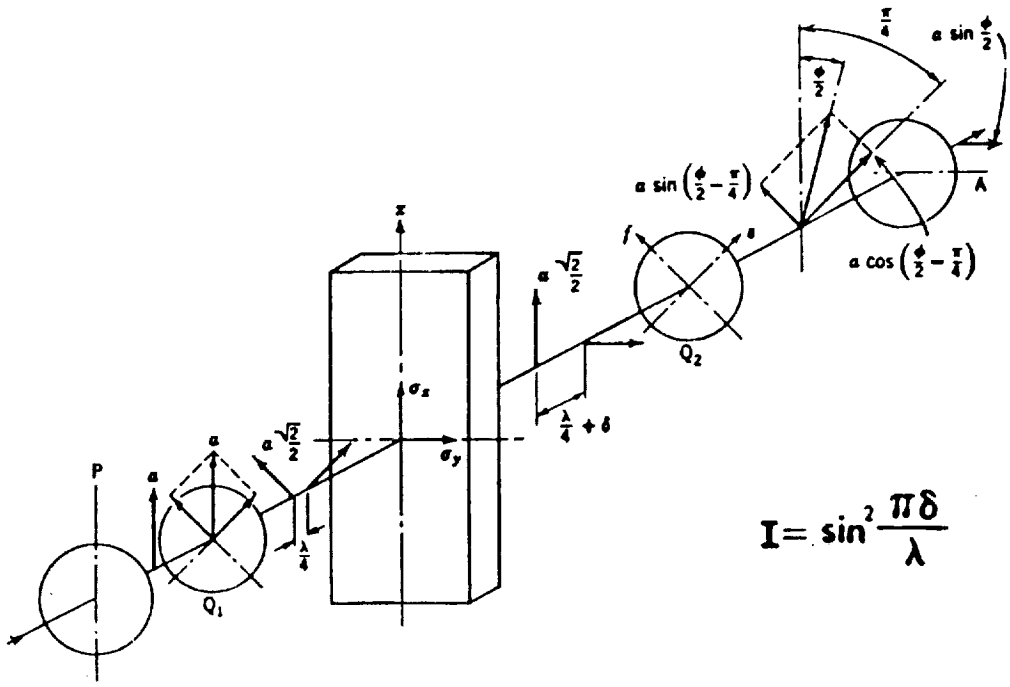

Fig. 2. Principle of a circular polariscope. Q_1 and Q_2 are quarter-wave plates; λ is wavelength; and s are axes of quarter-wave plate Q_2. Other symbols are as in Figure 1.

In the case of a Plane Polariscope, the intensity of light emerging will be:

$$I = a^2 \sin^2 2(\beta - \alpha) \sin^2 \frac{\pi \delta}{\lambda} \qquad (5)$$

Adding quarterwave plates in the path of light propagation transforms the instrument into a "Circular Polariscope". The emerging light intensity is now independent of the direction of principal stresses:

$$I = a^2 \sin^2 \frac{\pi \delta}{\lambda} \qquad (6)$$

or

$$I = a^2 \sin^2 \frac{\pi}{\lambda} C_B t (\sigma_x - \sigma_y) \qquad (7)$$

The expressions (5) and (6) shown above basically describe the relationship between the transmitted light intensity and the state of stress (σ_x, σ_y). (A more complete derivation of the transmitted light intensity equation see Ref. 5).

2.2. BIREFRINGENT SENSOR

The birefringence $n_x - n_y$ in a stressed material is proportional to the difference of principal strains or stress. The birefringent material becomes, therefore, a sensor responding to stress, or in a form of a transducer, to any action that can be translated into stress. For example, a cylinder filled with pressurized fluid responds to pressure, a column subjected to force can measure the force, etc.

The concept is used in the experimental stress analysis for photoelastic measurements of strains in models, and in a form of a photoelastic coatings for measuring of surface strains in structures.

The birefringent sensor is particularly suitable for measuring strains at elevated temperature, or more generally as a sensor for an elevated temperature transducer.

Since the sensor responds to the DIFFERENCE of principal strains $\varepsilon_1 - \varepsilon_2$, the strains due to the thermal expansion do not generate any response, and also, the thermal stresses due to the mismatch of coefficient of thermal expansion between the sensor and the transducer structure do not generate any "zero shift" or error.

The birefringent sensor was not used in the past because of the unavailability of a practical birefringence measuring technique.

2.3. TECHNIQUES OF MEASUREMENTS

Several methods are used to measure δ, depending upon the size of δ and also of the precision required.

a. Observation of the color pattern

When the crossed polarizer-analyzer is at 45° to the direction of stresses ($\beta - \alpha = 45°$) the emerging light intensity becomes:

$$I = a^2 \quad \sin^2 \frac{\pi \delta}{\lambda}$$

The brightness of emerging colors is modulated by the retardation δ, as shown in the above equation. Certain colors are better transmitted: ($\sin^2 \frac{\pi \delta}{\lambda} = 1$) or $\lambda = 1/2\delta$, $\lambda = 3/2\delta$, $\lambda = 5/2\delta$ while others are obstructed: ($\sin^2 \frac{\pi \delta}{\lambda} = 0$, or $\lambda = \delta$, 2δ, 3δ, etc.)

As result of this variable transmittance, the light emerging from a stressed item appears in colors, with the relation between the retardation δ and observed color shown in the Table 1.

TABLE 1 Color* Sequence Observed Versus Retardation Value

Color	Retardation δ nm
Black	0
Gray	150
White-yellow	250
Yellow	300
Orange (dark yellow)	450
Red	500
Indigo-violet (tint of passage #1)	570
Blue	600
Blue-green	650
Green-yellow	750
Yellow	850
Orange (dark yellow)	950
Red	1050
Indigo-violet (tint of passage #2)	1140
Green	1300
Green-yellow	1400
Pink	1500
Violet	1700
Green	1750

*The colors are affected by the spectral distribution of the light source, characteristics of polarizing filters, etc.

b. Compensator

The use of a compensator is by far the simplest method to measure δ. The compensator is a calibrated device, adding to the retardation produced by the specimen an equal retardation, but of the opposite sign. The result produced is zero, which can be easily recognized visually and objectively, since the light intensity becomes zero regardless of wavelength or color used. Various compensators are commercially available. The most popular models are:

"Babinet" or "Wedge" Compensator: The retardation varies along its length, and is readable on a calibrated scale attached to it.

"Babinet-Soleil" or "Double Wedge" Compensator: The retardation is constant within the transmitted light areas and can be adjusted (shifting wedges) by means of a lead screw. The position of the lead screw is factory calibrated, and displayed using a variety of means.

c. Rotating Analyzer Compensator

The analyzer A is rotated until a minimum light intensity is observed. The minimum light intensity occurs when:

$$\frac{\pi \delta}{\lambda} - \alpha = \pm N\pi$$

where α is the rotation angle.

The measured retardation is:

$$\delta = \left(\frac{\alpha}{\pi} \pm N\right)\lambda$$

All above techniques require direct visual access and a highly skilled engineer's time for measuring at a point. As a result of these difficulties, the measuring of stress using the photoelastic approach is restricted to special applications only.

3. SPECTRAL CONTENTS ANALYSIS METHOD OF MEASURING BIREFRINGENCE

The measuring of birefringence using the spectro-photometric approach was first proposed in 1984 by Redner (1). The system schematic is shown in Figure 3 below.

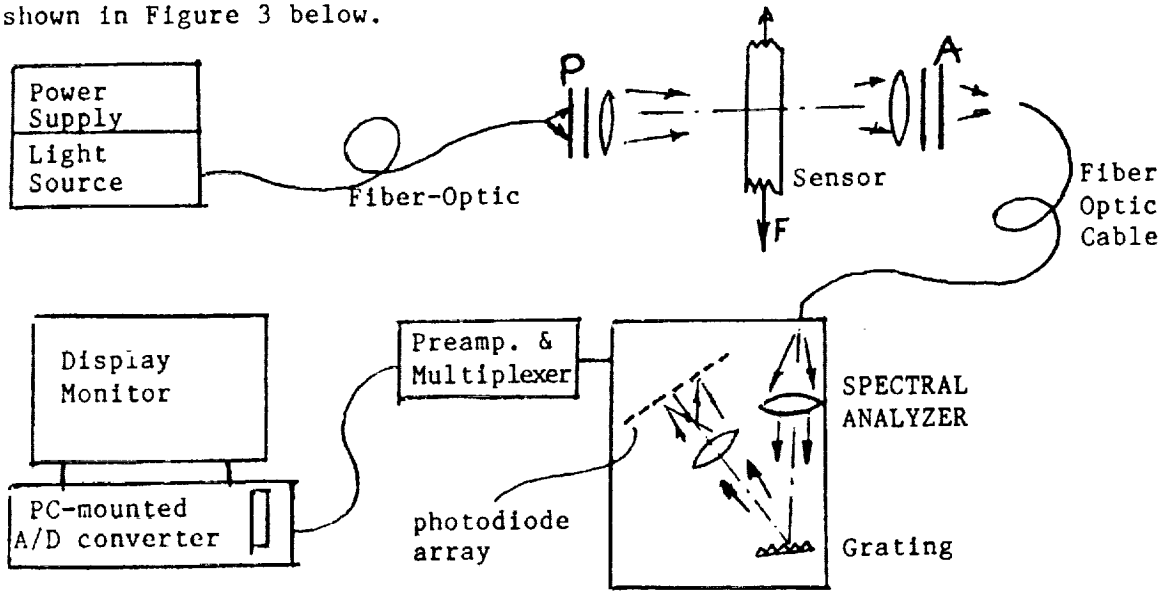

Figure 3. Spectral Contents Analysis System Schematic

This method permits point-by-point measurements of the retardation without prior knowledge of directions of principal stresses. The method considerably simplifies the optical set-up for automatic data acquisition, and is useful for both static and dynamic applications. The spectral-contents method uses white light and a broad range of spectrum. The performance of every element in a system is wavelength dependent. The spectral distribution of the light source emittance depends on the filament temperature and follows Planck's law. Each optical element (lenses, filters, quarterwave plates, model) transmits individually less than 100 percent. A combined transmittance $T(\lambda)$ (disregarding polarization effects) is a product of individual actions of these elements, and is also wavelength dependent. Finally, the conversion factor of the photoelectric detector-amplifier system is again wavelength dependent. The emerging light intensity can now be expressed as:

$$i(\lambda) = D(\lambda)\cdot I(\lambda) = D\cdot I_s(\lambda) \times T(\lambda) \times \sin^2\frac{\pi\delta}{\lambda} = S(\lambda)\cdot T_M(\delta,\lambda) \quad (8)$$

where $i(\lambda)$ is the measured photoelectric-current output, $S(\lambda)$ is the spectral factor of the overall system, and $T_M(\delta,\lambda)$ is the retardation dependent "spectral transmittance" of a photoelastic member placed in a circular polariscope, and $D(\lambda)$ is the photoelastic conversion factor.

$$T_M(\delta,\lambda) = \sin^2\frac{\pi\delta}{\lambda} \text{ (Dark Field)}$$
$$T_M(\delta,\lambda) = \cos^2\frac{\pi\delta}{\lambda} \text{ (Light Field)} \quad (9)$$

The equations above demonstrate that the sensor spectral transmittance T_M is modulated by the measured retardation. For illustration, Fig.4 shows T_M at various stress (retardation) levels. Conversely, when the transmittance curve T_M is established by spectral analysis, δ can be extracted using the measuring system and data analysis.

As shown in the schematic, the stress-modulated light emerging from the investigated point is channeled to the spectral analyzer functioning as a conventional spectro-photometer. Using a diffraction grating, the light is divided into several rays, each carrying a narrow band of frequencies. The beam is then refocused on a photodiode array, each photodiode measuring light intensity carried on its assigned central wavelength λ_j (m photodiodes in the array, $1 \leq j \leq m$). The photoelectric current $i(\lambda_j)$ can be measured and recorded.

Initially, a stress-free model is introduced using a light-field polariscope set up (polarizer and analyzer parallel). For $\delta = 0$ we have $T_M = 1$ and $i(\lambda) = S(\lambda)$. For each wavelength λ_j employed in the system, the measured current $i(\lambda_j)$ reveals the overall spectral factor $S(\lambda_j)$, calibrating the system. Once $S(\lambda)$ is established, the transmittance $T_M(\delta,\lambda)$ of a stressed model can be measured accurately. For each wavelength λ_j we have:

$$T_M(\delta,\lambda_j) = \frac{i(\lambda_j)}{S(\lambda_j)}$$

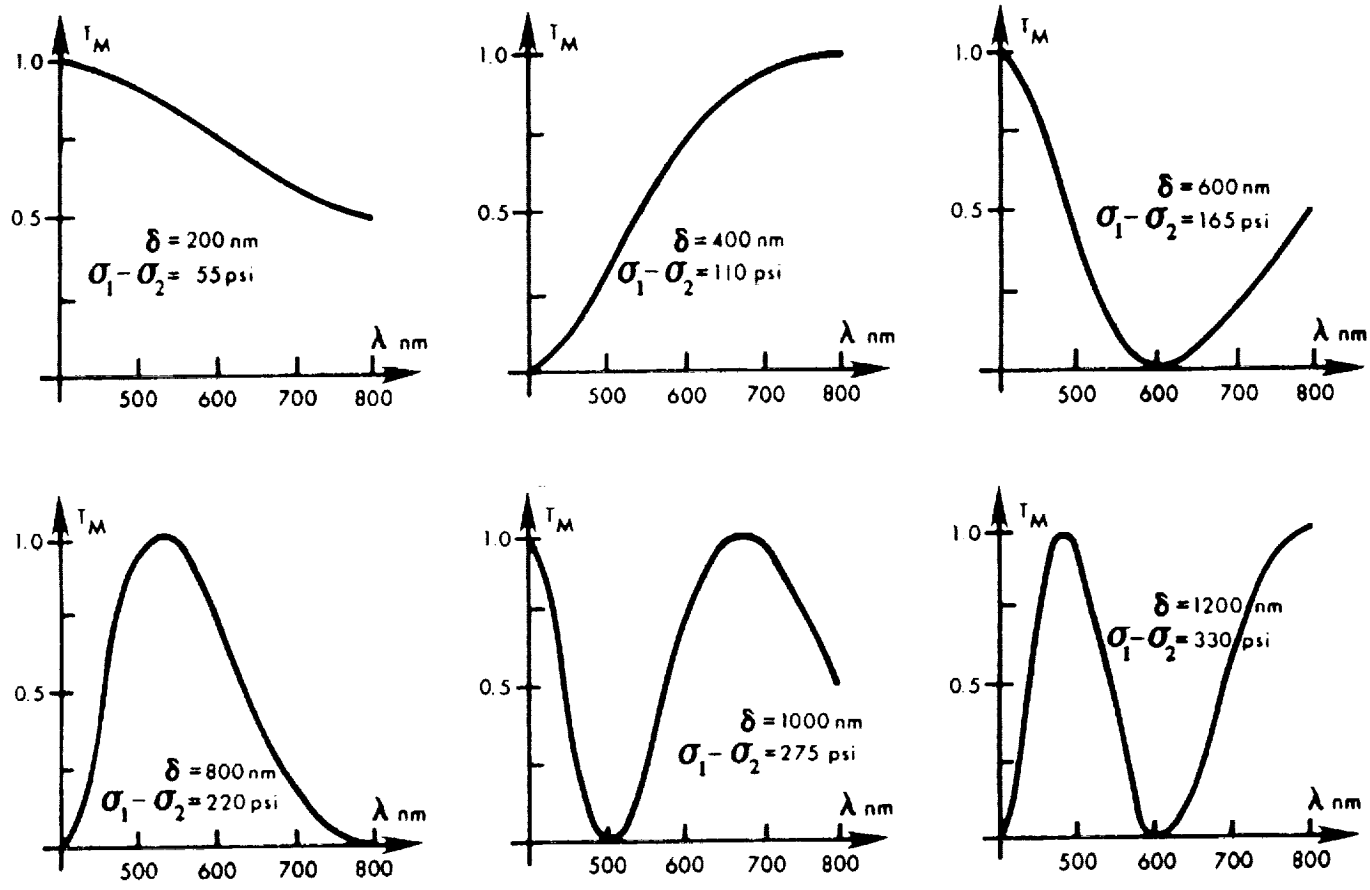

FIG. 4. SPECTRAL TRANSMITTANCE AT VARIOUS STRESS LEVELS

To eliminate possible errors, $S(\lambda)$ can be measured and updated repeatedly.

Some additional precautions observed in a spectrophotometer system should also be considered, including the "dark current" evaluation, polarizer efficiency, linearity, etc. These factors will affect the precision of the light-intensity measurements, but their influence on the precision of retardation measurements is small as a result of the curve-fitting procedure used in the data analysis.

3.1. DATA ANALYSIS--EXTRACTING RETARDATION FROM TRANSMITTANCE MEASUREMENTS

The measured current $i(\lambda_j)$ from photodiodes reveals the sensor's transmittance $T_M(\delta, \lambda_j)$ as a spectral signature of the existing state of stress. By combining eqs. (8) & (9), the following relations can be written for a dark-field polariscope ($1 \leq j \leq m$).

$$\sin^2 \frac{\pi\delta}{\lambda_j} = T_M(\delta,\lambda_j) = \frac{i(\lambda_j)}{S(\lambda_j)} \qquad (10)$$

Solving these equations for δ_j we have:

$$\delta/\lambda_j = \pm\frac{1}{\pi}\sin^{-1}\sqrt{\frac{i(\lambda_j)}{S(\lambda_j)}} + n_j = n_j \pm f_j = Nj$$

or

$$\delta = N_j\lambda_j = (n_j \pm f_j)\lambda_j \qquad (11)$$

This relation is typical of a dark-field polariscope, where N is the fringe order, n is an integer and represents the "full order" and f is the fractional order.

We have a system of m equations (10) containing m + 1 unknowns, the integer fringe orders n_j and δ.

The method that is most suitable for solving this system is a computer-performed search for a curve that best fits the experimental data. Given a set of m data points $T(\delta, \lambda_j)$, within the range of measurements there is only one value of X that for all λ_j satisfies the relation:

$$\sin^2 \frac{\pi X}{\lambda_j} - T_M(\delta,\lambda_j) = 0 \qquad (12)$$

The computer solves this equation easily. The root of this equation X is the measured retardation δ, and the curve $T_M = \sin^2 \frac{\pi X_o}{\lambda}$ best fits all experimental points.

3.2. COMPUTER-BASED SOLUTION OF THE SPECTRAL CONTENTS ANALYSIS EQUATIONS

In the Phase I research, several approaches were evaluated to assess their merits, speed of solution, and potential problems.

Graphically, the solution is illustrated in the Figure 5 below. Given "m" experimentally acquired light intensities at λ_j, which of the transmittance curves (Figure 4) fits the best?

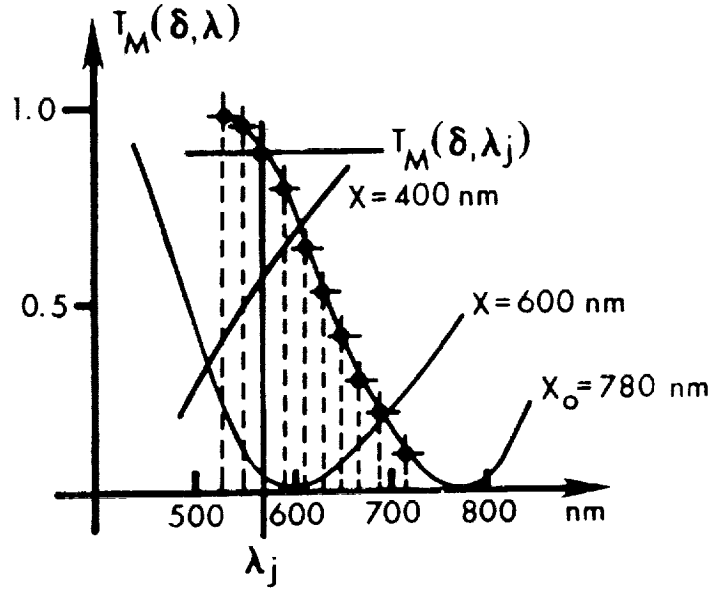

Figure 5. Matching Transmittance Curve to Data

3.2.1. Data Base Search Approach

As an alternative approach for extracting the retardation value from measured spectral content of the signal, the data base search was tested. During initialization of the system, the present value of retardation in a specimen can be achieved by a controlled loading. The procedure of the data base creation was to apply known load, which results in the known retardation, and acquire light intensity by all photodiodes (maximum number 16) and store it in an array 16 elements wide. This loading procedure continued until an array of 200 X 16 was built and permanently stored on a disk.

To extract value of retardation during actual test, the acquired information (16 photodiode) was compared by each of the 200 columns in the data base and difference between actual reading and corresponding position in the data base was calculated and compared to the present limit. If the difference was less than the limit, a value of 1 was assigned to the flag, otherwise - flag was set to zero. This procedure is repeated for each photodiode and all values of flag were added.

After going through all columns, 200 flags were calculated. Their values were ranging from 0 to 16. The flag with highest reading denotes the position of the solution. In case of more than two flags giving the same maximum value, the preset limit was halted and procedure was repeated.

3.2.2. The Newton-Raphson Approach

Use of the Newton-Raphson approach for extraction of the retardation was suggested by Sanford (3). To account for experimental errors and some systematic errors, the finite form of the equation (12) was modified to include additional parameters responsible for constant shift and rotation of the spectral response plot. However, some difficulties were encountered and two separate techniques were used for extracting of retardation lower than 2π and higher than 2π.

Here, the problem was approached as follows: The light intensity as acquired by each diode is presented as in eq. (15) with additional unknown scale factor β, which should take care of some minute changes in the calibration parameter $I_o(j)$ because of light source and amplifiers instability. Let us create a function $g(\delta,\beta)$.

$$g_j(\delta,\beta) = I_j(\delta) - I_j^m \qquad (13)$$

Taylor's series expansion gives:

$$(g_j(\delta,\beta))_{k+1} = [g_1]_k = \left(\frac{\partial g_i}{\partial \delta}\right)_k \Delta\delta + \left(\frac{\partial g_i}{\partial \beta}\right)_k \Delta\beta, \qquad (14)$$

where k is the iteration stop number

and $\Delta\delta$, $\Delta\beta$ are corrections to the initial guess.

Since $g_j = 0$ will provide solution, the following set of equations will result:

$$-[g_j]_k = \left(\frac{\partial g_j}{\partial \delta}\right)_k \Delta\delta + \left(\frac{\partial g_j}{\partial \beta}\right)_k \Delta\beta \qquad (15)$$

or in matrix form

$$[D] * (\Delta) = \{G\} \qquad (16)$$

System of equations (15) is solved for the unknown increments $\Delta\delta$ and $\Delta\beta$. This process is repeated until the preset convergence limit is achieved.

The main problem with such technique is that the initial guess has to be supplied for procedure to start. If the initial guess is far from actual solution, no convergence is achieved. (The initial guess can be supplied from the above described "Error-summation approach".) One can run it in relatively coarse increments and the obtained approximate solution can be used as an "initial guess".

To verify this approach, several increments were tested for wide range of measured retardation (0-5000nm). It was found, that increments of 40-50nm always provided correct solution with prescribed accuracy.

3.2.3. Error-Function Minimization Approach

Value of $I_i(\delta)$ can be calculated for each possible retardation δ within the considered range, and compared to the actually measured value I_j^m. Given a set of n data points I_j^m within the range of measurements there is only one value of δ that satisfies for EACH photodiode j the relation:

$$I_j(\delta) - I_j^m = 0 \qquad (17)$$

Where I_j is the photoelectric current measured by a photodiode observing λ_j.

To solve these n equations, the error-summation approach can be used. The search is made for value of δ that will minimize the error function $E(\delta)$.

$$E(\delta) = \sum_{j=1}^{n} (I_j(\delta) - I_j^m) = \text{minimum} \qquad (18)$$

Equation 18 is solved by a simple search over the range of possible retardations from 0 to 5000nm in 10nm steps.

The range (5000nm) and step (10nm) can be selected arbitrarily, in accordance with the range and the need of resolution of the results that are needed. It is possible to store an array of calculated $I_j(\delta)$ for any number n of photodiodes and any increment of δ. The search for the solution of equation (18) can be considerably accelerated when:

a) The selected range decreases

b) The number of photodiodes decreases

c) The step of the search increases

In practice, a coarse search in steps of 50nm proved acceptable, with the final search around the approximate value proceeding in smaller steps, or using a linear approximation.

As a result of an extensive evaluation carried out in the Phase I research, the error function minimization was found to be the fastest and most reliable algorithm and was retained for the SPECTRAL CONTENTS method throughout the Phase II research. The error function uses relatively coarse steps in the search for the solution, and a technique of linear interpolation was used to enhance the system resolution, without sacrificing the speed of response.

3.3. FACTORS AFFECTING THE TRANSMITTED LIGHT INTENSITY

The equations (6) and (7) are not considering all factors influencing the transmitted light intensity. In addition to the stress-related transmittance modulation other factors must be considered, including:

- Dispersion of birefringence
- Inaccuracies of quarterwave plates
- Efficiency of polarizers

- Finite wavelength perception of an array element
- Temporal changes of the transmittance, opacities, and source emission.

The final expansion that was used in the data-acquisition system incorporated the following consideration.

3.3.1. Dispersion of Birefringence

Some materials exhibit a significant dispersion of birefringence within the band $\Delta\lambda$ selected. Material calibration must be performed to assess if indeed the dispersion is sufficiently large to justify the correction procedure proposed here. If C_o is the material constant using a "nominal" wavelength λ_o, and at an arbitrary wavelength λ the constant becomes C, it follows from eq. 4 that:

$$(\sigma_1 - \sigma_2)t = \frac{\delta_o}{C_o} = \frac{\delta}{C} \tag{19}$$

The equation for light intensity and transmittance can be rewritten as follows:

$$T_M(\delta, \lambda_j) = \sin^2 \frac{\pi\delta}{\lambda_j} = \sin^2 \frac{\pi}{\lambda_j} \frac{\delta_o C}{C_o} = \sin^2 \frac{\pi\delta_o}{L_j} \tag{20}$$

The retardation δ_o can be considered as constant, independent of wavelength, but a dispersion corrected wavelength L_j must be introduced:

$$L_j = \frac{\lambda_j C_o}{C} \tag{21}$$

For best accuracy, each material should be calibrated within the range to be used. We have calibrated the most useful material and found the dispersion sufficiently small to justify a linear approximation for the function C_o/C.

A typical result of calibration is shown in Figure 6 below.

The "nominal" wavelength, 570 nm, does not have to be contained within the range of wavelengths used for measurements, provided the calibration constant is properly measured.

3.3.2. Quarterwave Plate Error

The influence of quarterwave plate mismatch in the polychromatic polariscope is not negligible. Assume that the quarterwave plate is selected for the midrange of the employed band λ_M, its retardation is $\frac{\lambda_M}{4}$, and the phase shift is $\frac{\pi}{2}$. For other

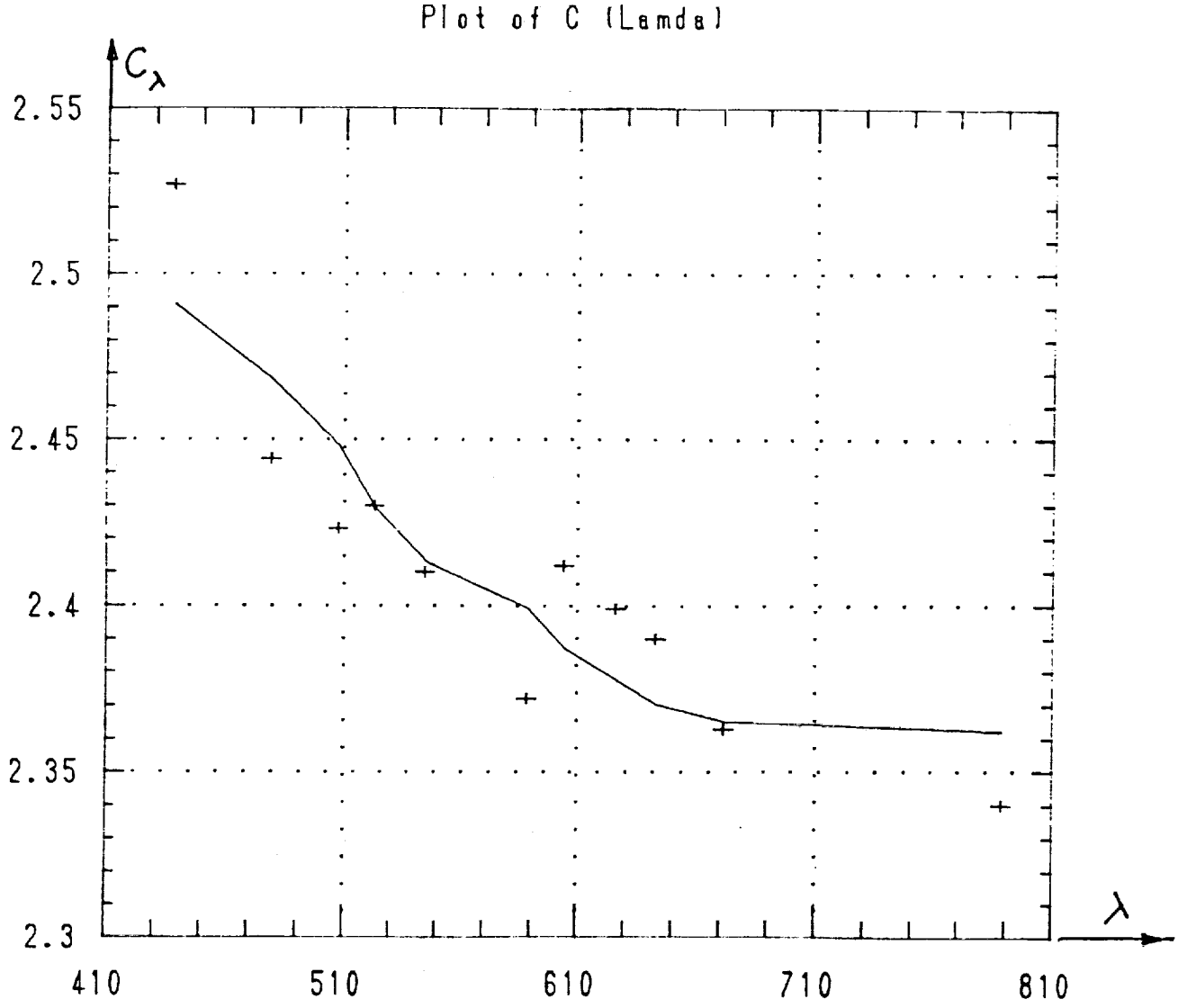

Figure 6. Dispersion of Birefringence

wavelengths, λ_j, the phase shift is different and the phase error becomes:

$$e_\alpha = \frac{\pi}{2}\left(\frac{\lambda_M}{\lambda_j} - 1\right) \qquad (22)$$

The effect of the error in the quarterwave plate on the light intensity and transmittance becomes:

$$T_M(\delta, \lambda_j) = \sin^2 \frac{\pi\delta}{\lambda_j}\left(1 - \sin^2 2\alpha \sin^2 e_\alpha\right) \qquad (23)$$

This equation illustrates that the error introduced depends on the angle α between the direction of stresses and the orientation of the quarterwave plates. In those instances where the quarterwave plates are parallel to the direction of stress (α = 0 deg.) there is no error. Maximum errors occur when α = 45 deg.

It is possible to partially correct for the quarterwave-plate mismatch. Since the direction α is not usually known, an average value of $\sin^2 2\alpha = 0.5$ can be used, partially offsetting the error. This correction can be altogether disregarded if in the final analysis and evaluation only a narrow band of λ_j is used. The actual procedure depends on the programming steps used.

3.3.3. Photodiode Dimensions

The photodiode array used in this research program was a 32-element lineary array. The dispersing grating was adjusted to provide approximately 320 nm dispersion over the length of array and each element was receiving the illumination over a 10 nm spectral band.

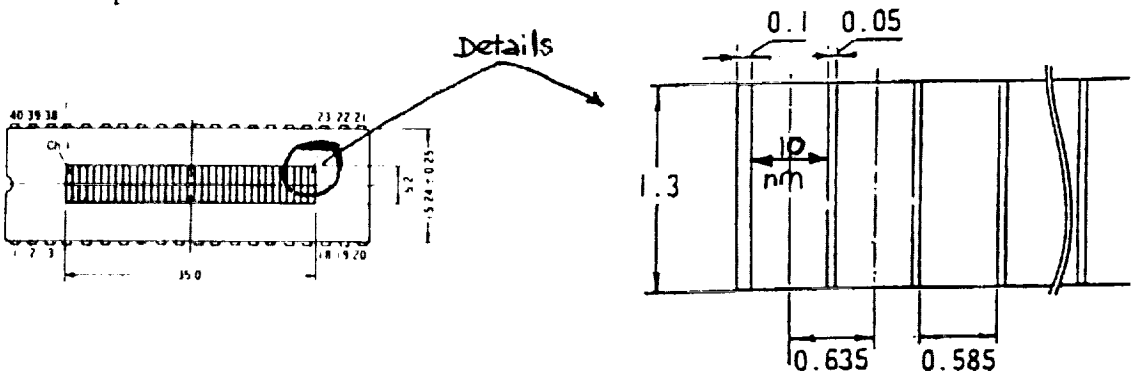

To properly account for the non-monochromatic perception of each element, the light intensity must be integrated over the spectral width.

$$I_c = \frac{1}{\Delta\lambda}\int_{\Delta\lambda} I_\lambda(\lambda)\,d\lambda$$

In practice, numerical integration was used. Each element was divided in five increments of 2 nm and the summation was carried out numerically. This correction for the physical dimension of each photodiode is particularly significant when large retardation (above 2000 nm) is measured. In measuring small retardation, it is not essential, but contributes to an improvement of accuracy.

3.3.4. Efficiency of Polarizers

Commercial polarizers are not 100% efficient and the ratio of polarized/unpolarized light (or efficiency) is strongly wavelength dependent.

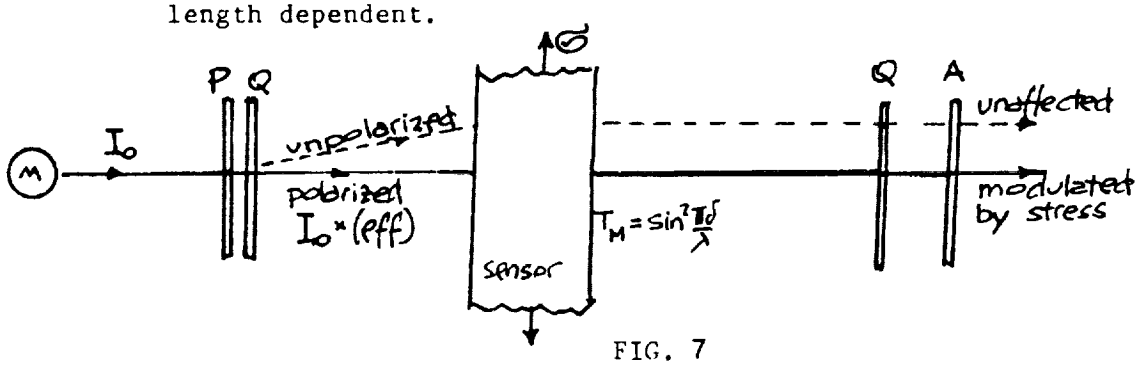

FIG. 7

The unpolarized light emerges unaffected by the stress in the sensor, while the polarized light is modulated by the spectral transmittance term T_M.

The detector receives both components:

$$I_\lambda = I_{o\lambda} \cdot (eff) \cdot \sin^2 \frac{\pi\delta}{\lambda} + I_{o\lambda}(1 - (eff)) \qquad (24)$$

3.3.5. Temporal Changes

Over a period of time, the light bulb darkens, some of the optical components degrade or their surfaces deteriorate. In the first approximation, it can be considered that the increasing opacity of the system is wavelength independent, and the opacity becomes a constant factor (see "witness diode" below).

3.3.5. Light-Intensity Expression

Considering all the influences above, the expression to evaluate the light intensity incorporated all corrections shown above, yielding:

$$I_{\lambda_j} = \int_{\Delta\lambda} \left[I_{o\lambda} (eff) \sin^2 \frac{\pi\delta}{\lambda} \cdot \frac{C_\lambda}{C_o} \left(1 - \sin^2 2\alpha \sin^2 \theta_a\right) \right] d\lambda + I_{o\lambda}(1 - eff) + D(j) \qquad (25)$$

where D_j is the "dark" current output measured with the light source turned off.

4. TECHNICAL OBJECTIVES

During the Phase I research work on the Spectral Contents Analysis (SCA) method, a conceptual prototype was assembled. It was demonstrated that the SCA method is feasible, accurate, and offering a potential of usefulness.

The objectives of the Phase II research reported here were to develop a working instrument system based on the SCA concept, that would fully utilize the potential of this method. In particular, the following objectives were specifically targeted:

- Investigate and evaluate materials suitable for use as a birefringent sensor, capable to operate at temperatures up to 1000° C.
- Define the sensor geometry (for bonded and unbonded configurations).
- Develop a "state-of-the-art" data acquisition system based on SCA, with capability of:
  - High-sensitivity measuring of birefringence
  - Multipoint data acquisition
  - Dynamic measurements
  - Self-calibration automated readout feature
  - High-temperature operation
  - Develop software (a program) operating the system

Test the system to evaluate its capabilities and performance.

5. SENSOR MATERIAL AND GEOMETRY

Virtually all transparent materials can be considered for use as a birefringent sensor, including some materials that are transparent in infrared range only, such as silicon, germanium, and galium-arsenide.

The choice of a sensor material suitable for a particular application must be based on:

a) Strain-optic response
b) Compatibility with the environment
c) For a bonded-sensor, compatibility of thermal expansion

In room-temperature applications, polycarbonate and epoxy resin are usually the best choices. Their strain-optic response is excellent (see table II) and the birefringence-dispersion for epoxy compound is very low, making it the best choice for a bonded sensor.

The candidate materials for elevated temperature use are shown in the Table III. Although the choice appears very broad, one must limit the consideration to readily available materials in a stress-free state, birefringence-free.

In this research, our effort concentrated on fused silica. Fused silica offered all the required features, including:

- Good mechanical properties, (up to 1100° C)
- Acceptable (although low) k-factor
- Availability in all desired geometries
- Moderate cost

The fused silica sensor can be used both as an unbonded sensor and as a bonded gage. The unbonded birefringent sensor configuration includes a pressure sensor, load cell, or any desired transducer function.

Strainoptic has designed and tested a pressure sensor using fused-silica unbonded diaphragms for measuring high-temperature gas pressure up to 500 psi.

The bonded birefringent sensor concept is well known and commonly used (photoelastic coating) (5). In selecting the bonded sensor for elevated temperature application, the matching of the coefficient of linear expansion is the key consideration. In most instances, the sensor should preferably have a coefficient of expansion slightly higher than the subtrate, thus developing a compressive biaxial stress when heated.

The evaluation of the bonding agents for cementing of the sensor was carried out using AREMCO cements, following the manufacturer's suggested application procedures.

TABLE II

STRAINOPTIC ACTIVITY OF MATERIALS

Material	Strainoptic K factor	C_B
Polycarbonate	.15	82
Epoxy	.10	54
Glass (soda-lime)	.13	2.65
Zerodur	.14	3.0
Fused Silica	.16	3.4
Silicon	3.1	20
Germanium	4.0	33

TABLE III. CANDIDATE OPTICAL SENSOR MATERIALS

Material	Formula	°C Melting Point	Crystalline Structure	Index of Refraction
Aluminum Nitride	AlN	> 2200	hexagonal	
Sapphire	Al_2O_3	2053	rhombohedral	1.765
	Be_3N_2	2200	cubic	
	CaO	2580	cubic	1.838
	$CaZrO_3$	2550	monoclinic	
	CeO_2	2600	cubic	
Spinel	$MgAl_2O_4$	2135	cubic	1.723
Periclase	MgO	2800	cubic	1.736
Silicon Carbide	SiC	2600	hexagonal or cubic	2.645 2.697
Silica	SiO_2	1800	amorphous	1.456
Zirconia	ZrO_2	2700	monoclinic below 1000 C Cubic above 1000 C	
Zircon	$ZrSiO_4$	2550	tetragonal	1.92-1.96 1.97-2.02

The tables 4 and 5 show the selection chart of ceramic cements for a variety of applications. The thickness t of the bonded fused-silica sensor must be selected in accordance with the measured strain level. The strains are related to the measured retardation by the equation 3. (where 2x t is used to account for double pass).

$$E_1 - E_2 = \frac{\lambda}{2tK}$$

For a given strain range S, and retardation range δ (typically 100 nm or more) the minimum thickness t becomes:

$$t = \frac{\delta}{2SK} - \frac{100 \times 10^{-9}}{2 \times S \times 0.14}$$

As example, for measuring 10,000 psi in steel ($S = 330 \times 10^{-6}$) a thickness of 1 mm (.040") is suitable. For measuring higher strains, smaller thickness is needed.

Using a silicon sensor (very high strain-optic activity) 0.1 mm thickness will provide the same response.

TABLE IV

AREMCO HIGH TEMPERATURE CERAMIC ADHESIVE PROPERTIES*

PROPERTY	503 Ceramabond	516 Ultra-Temp	552 Ceramabond	569 Ceramabond	571 Ceramabond	618 Ceramabond	632 Ceramabond	633 Ceramabond
Temperature Limit - °F	3000	4400	3000	3000	3200	1850	1200	2100
Major Constituent	Al_2O_3	ZrO	Al_2O_3	Al_2O_3	MgO	Silica	Mica	Alumino Silicate
Volume Resistivity (ohm-cm @ RT)	10^9	10^8	10^8	10^9	10^9	10^9	10^9	10^9
Volume Resistivity (ohm-cm @ 1000° F)	10^5	10^4	10^4	10^5	10^5	10^5	10^5	10^4
Thermal Expansion (in/in/°F x 10^{-6})	4.0	4.1	4.3	4.2	7.0	33	5.0	3.0
Thermal Conductivity (BTU/FT²/HR/IN/° F)	192	60	192	192	218	12	3	8
Dielectric Strength (volts per mil @ RT)	253	250	250	256	255	200	250	80
Dielectric Strength (volts per mil @ 1000° F)	240	80	80	100	100	180	200	60
Hardness (Mohs Scale)	6	6.5	6-8	6	5.5	N/A	3	5
Porosity (after curing) %	< 1	< 1	< 1	< 1	< 1	< 1.8	< 1	< 3
Moisture Resistance	Good after 700° F firing	Good	Excellent after 700° F firing	Excellent	Excellent	Good	Good	Good
Oxidation Resistance	Excellent	Excellent	Excellent	Excellent	Excellent	Excellent	Excellent	Excellent
Alkali Resistance	Fair	Excellent	Excellent	Excellent	Excellent	Good	Good	Good
Acid Resistance	Excellent attacked by HF	Good attacked by HF & H_2SO_4	Good attacked by conc. HF	Good attacked by HF	Fair attacked by HF	Good	Good	Good
Solvent Resistance (organic)	Excellent	Excellent	Excellent	Excellent	Excellent	Excellent	Excellent	Excellent
Shelf Life	6 months	6 months	6 months	6 months	6 months	6 months	6 months	6 months
Cure Guide	Air Dry + Heat	Air Dry + Heat	Air Dry + Heat	Air Dry	Air Dry + Heat	Air Dry + Heat	Air Dry + Heat	Air Dry + Heat

TABLE V

CERAMIC ADHESIVE SELECTOR CHART*

MATERIAL	CTE x 10^{-6} in/in/°F	AREMCO HI-TEMP CERAMIC ADHESIVES							
		503	516	552	569	571	618	632	633
ALUMINUM	15.01					•			
BRASS	10.2					•			
COPPER	9.3					•			
INCONEL	6.4		X	X	•	X			
KOVAR	2.6		X	•	X	X			X
MOLYBDENUM	2.9		X	X	•				X
NICKEL	7.2		X	X	X	•			
PLATINUM	4.9	X	X	X	•	X		X	
STAINLESS STEEL 302	9.6		X	X	X	•			
STEEL (1010)	6.5		X	X	X	•			
SILICON	1.6	X	•	X	X				
SILVER	10.6					•	X		
TANTALUM	3.9	X	X	X	•	X		X	
TUNGSTEN	2.5		X	X	•			X	
ALUMINA (98%)	4.4	•	X	X	X	X			
BERYLLIA (95%)	4.6	•	X	X	X	X			
BORON NITRIDE	4.17	•	X	X	X				
GLASS (Borosilicate)	1.80	•	X	X	X				
GRAPHITE*	4.3	•	X	X	X	X			
MICA	22	•	X	X	X		X	•	
MULLITE	3.0	•			X				X
QUARTZ	31	•			X		•		
SAPPHIRE	4.2	•	X	X	X	X		X	
STEATITE	3.99	•	X	X	X			X	
ZIRCONIA	5.6	X	•	X	X	X			

*AREMCO Products, Inc., Technical Bulletin #M2

6. DEVELOPMENT OF DATA ACQUISITION SYSTEM BASED ON SPECTRAL CONTENTS ANALYSIS METHOD (SCA)

The feasibility of the system and the initial concept was demonstrated in the Phase I research. During this feasibility program, a simple system (Figure 8) was assembled and demonstrated.

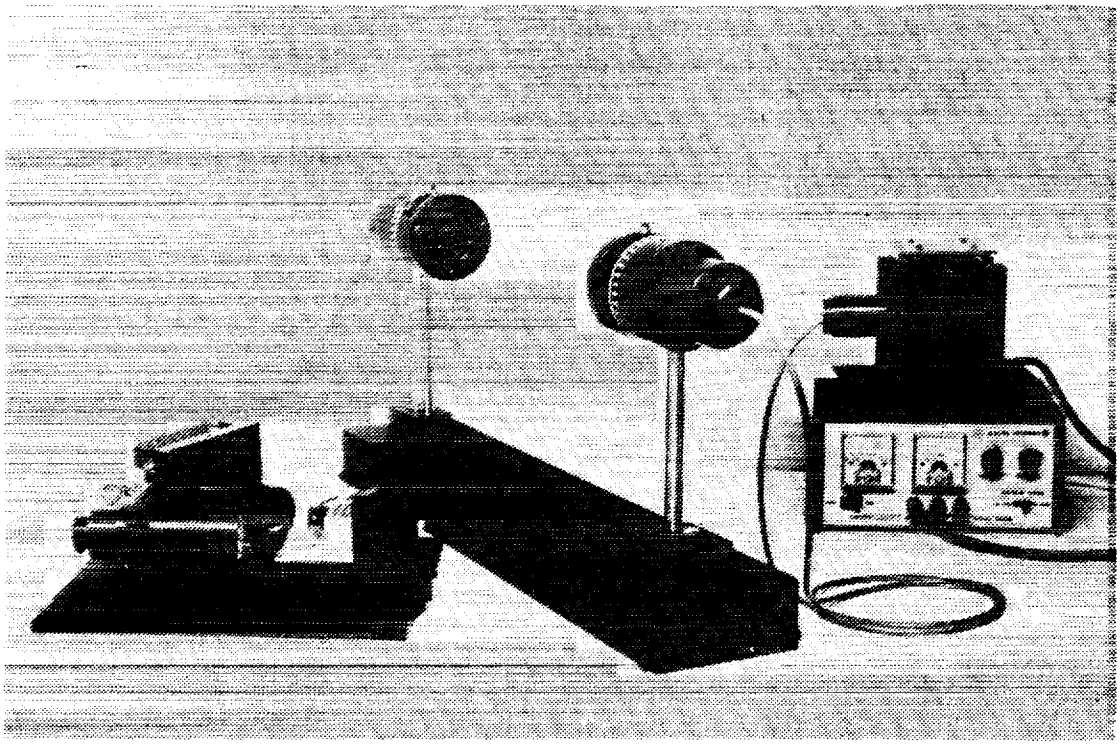

Figure 8. Phase I "Feasibility" System

The objective of the Phase II was to develop an operational system, capable of measuring the output from a birefringent sensor, including:

- Self-calibrate capabilities
- Multi-point data acquisition
- Fiber-optic data transmission
- Capability at measuring small strains
- Data acquisition at elevated temperature

All the above objectives were reached and the system was tested to demonstrate all the operations.

6.1. POLARIZER ANALYZER PROBES

Figure 9 Illustrates the polarizer and analyzer probes designed, assembled, and used throughout the Phase II program.

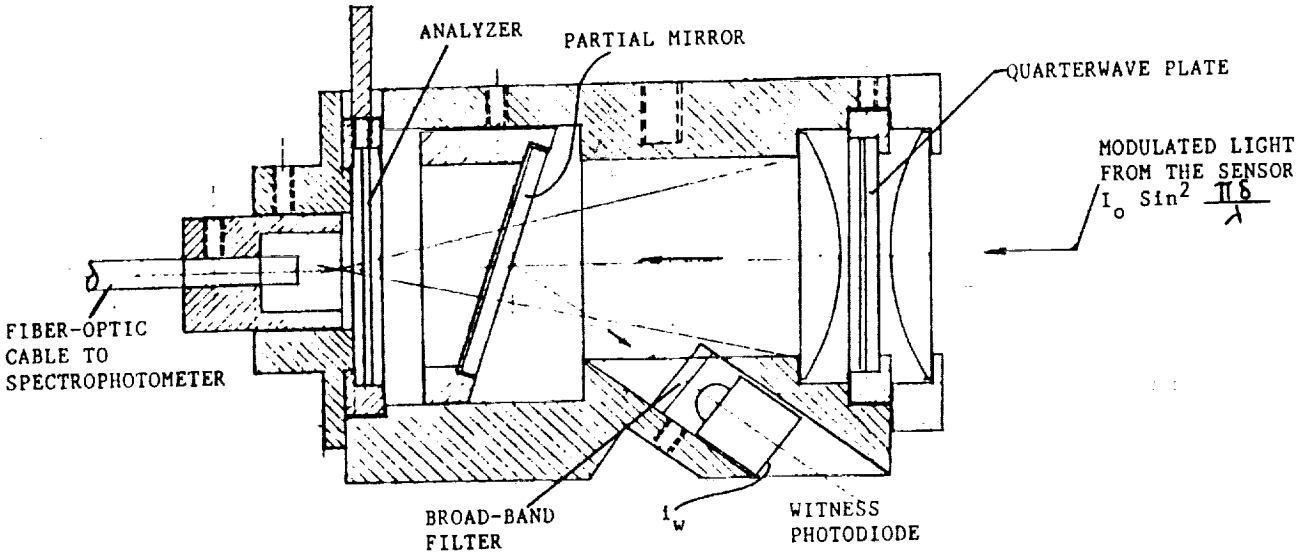

Figure 9a. Analyzer Probe

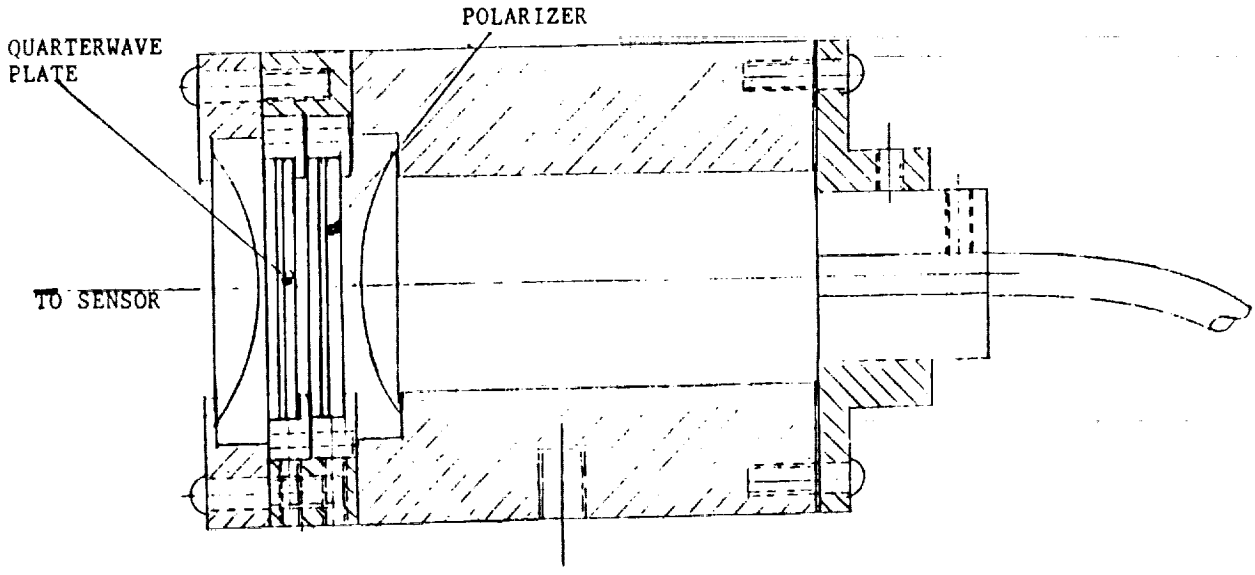

Figure 9b. Polarizer Probe

The size of the probes can be changed, depending on the application conditions, in particular, a different design is needed when reflection rather than transmission mode is used, or when high-temperature performance is required. Figure 10 below shows the probe design ("penetrator") for use at elevated temperature for operation at 1000° C.

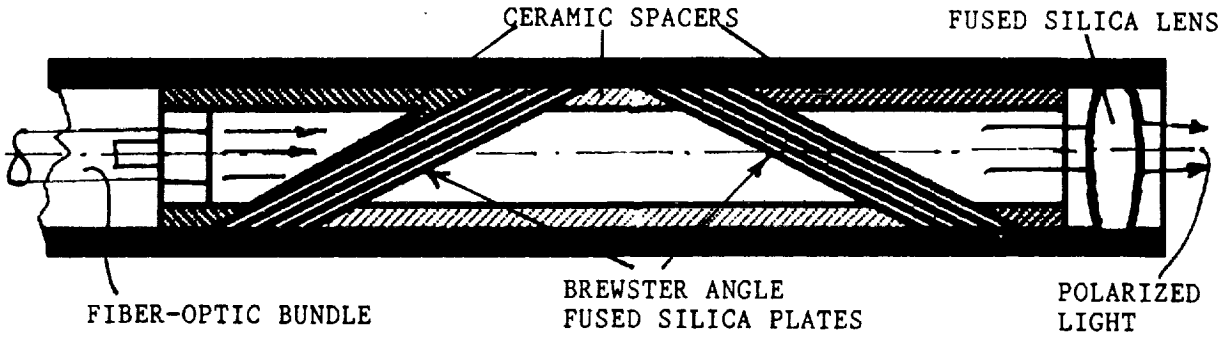

Figure 10. Penetrator

6.1.1. The polarizer itself is the most important element, affecting the system performance, mostly in the elevated temperature environment. For temperatures below 250° F, commercial polarizers were found satisfactory.

Since the SCA method encompasses a broad spectral range, the efficiency of polarizers and their ability to cover the range of wavelength from 480 nm to 850 nm was tested.

The following polarizers were evaluated:

a. Polaroid* polarizers, manufactured by Polaroid Corporation (Cambridge, MA).

   Type HN 22 and HN 32

b Acrylic-laminated polarizers made by American Polarizer (Reading, PA)

c. Crystal (calcite) (Carl Lambrecht, CVI Corp., and others).

d. Brewster angle polarizer

e. Polarization maintaining fiber-optic cables

*Polaroid is a trademark of Polaroid Corporation.

For applications at temperatures not exceeding 250° the dichroic polarizer manufactured by American Polarizers was found most advantageous, since it offered:

- Better uniformity of properties
- Broader spectral range
- Better efficiency at the red and near-infrared range of the spectrum that is essential in the SCA system

The polaroid HN22 is a satisfactory substitute for operation in a limited spectral range with a maximum 200 nm spectral width.

For elevated temperature range, an extensive search was conducted to determine the best approach. The available options included:

- Calcite cube glass-Thompson polarizers, available from Carl Lambrecht (and other manufacturers)
- Beam splitter cubes (using coating on interfaces)
- Pellicle polarizers
- Air-spaced cubes (Wollaston)
- Brewster-angle plates (or stack of plates)

Since our objective was set at temperatures of 1000° C and above, most of the cemented crystal and pellicle polarizers could not be considered.

The air-spaced cubes had a very narrow effective aperture, and also a narrow wavelength bandwidth, not compatible with the SCA operation. Our choice was narrowed to the Brewster angle stack.

In order to evaluate the degree of light polarization based on Brewster's angle, an experiment was set up, shown schematically on the drawing, Figure 11.

The light source providing a parallel beam of light was used. In the path of the light beam a stack of plates (fused silica) was placed, as shown on the Figure 11 (at Brewster angle). The light intensity transmitted through the stack of plates and reflected by the plates were measured by a photodiode. The photodiode output was first amplified and then displayed on a voltmeter. Between the plates and the light source an optical filter was set. The filter was cutting off undesired light, which is not included in the wavelength range considered.

ORIGINAL PAGE IS
OF POOR QUALITY

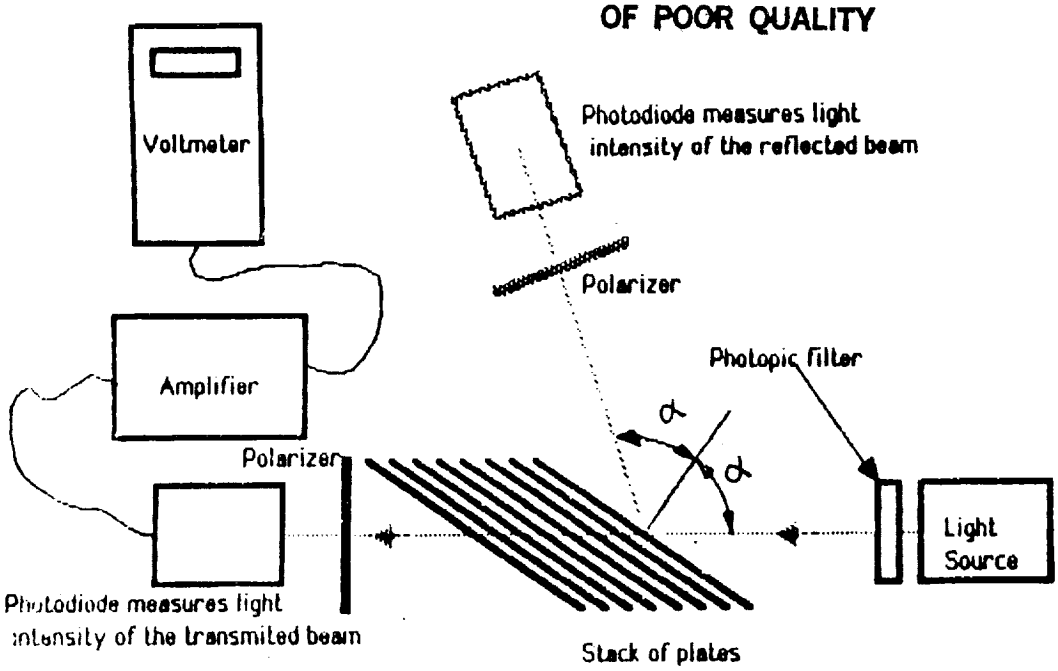

FIGURE 11

Calculation of the Brewster angle:

$\alpha = tg^{-1} n$ — n - index of refraction for fused silica

$\alpha = 55.6°$ — For our application n = 1.46

The results of measurement are shown in the table below. Experiments were carried out for one plate, stack of 4, 6 and 10 plates.

		Photodiode output					
		No Pol.	Parallel Pol.	Perpendic. Pol.	No Light	Polariza. Efficiency	Energy Efficiency
1 Plate	Throughtran.	-4.95	-2.07	-1.58	0.03	23%	9.10%
	Reflection	-0.45	-0.332	0.008	0.021	96.30%	6%
4 Plates	Throughtran.	-2.65	-1.37	-0.59	0.014	57%	14.50%
	Reflection	-1.09	-0.81	0.012	0.019	99.20%	15%
6 Plates	Throughtran.	-2.75	-1.52	-0.48	0.015	68.40%	19.30%
	Reflection	-1.19	-0.88	0.008	0.016	99.1%	16.50%
10 Plates	Throughtran.	-2.33	-1.48	-0.24	0.014	83.80%	23%
	Reflection	-1.48	-1.1	0.007	0.015	99.30%	20.60%

Numbers in the table show the voltmeter reading, proportional to the light intensity. The first column ("No Pol.") shows the reading without the polarizer in between the photodiode and the plates. The second and third columns represent light intensity with the polarizer inserted between the plates and photodiode. First the polarizer was rotated to get maximum reading (2^{nd} column - "Parallel Pol."). For the next column (3^{rd} column - "Perpendicular Pol."), the polarizer was rotated to get minimum reading. The last column ("no light") represents voltage shown on the meter when the light source was turned off.

Also, the following measurements were taken: without the stack of plates and the polarizer as shown in the Figure below, and with only the polarizer in between the light source and the photodiode. The efficiency was calculated as ratio polarized/ available light.

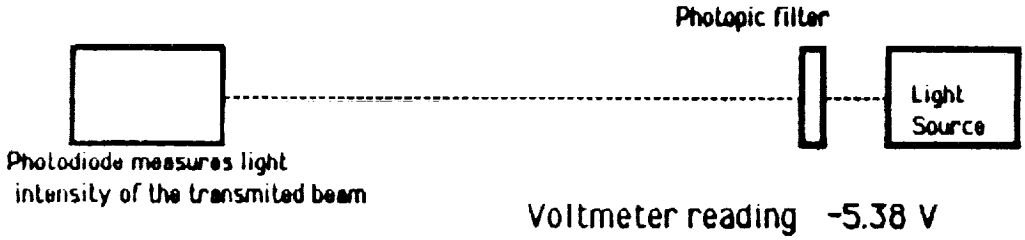

Voltmeter reading -5.38 V

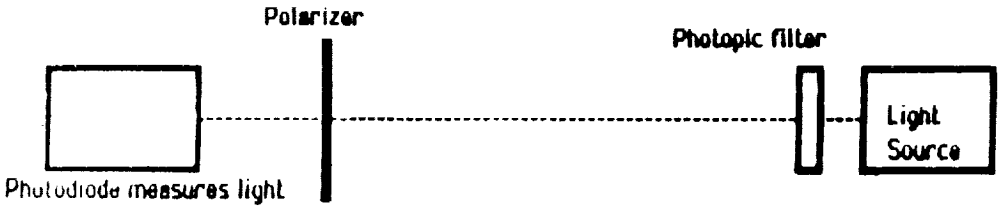

Voltmeter reading -2.02 V

As it can be seen, the "stack of plates" concept can be used to design an efficient polarizer, using reflected or transmitted light. The reflected light shows better efficiency, and should be used whenever the geometry of the sensor makes it practical.

The penetrator probe for high-temperature applications was based on the "stack of plates".

The "polarization maintaining" fiber-optic guides were considered for future use. At the present time, their use was not called for, since these guides are mounted in plastic jackets and are not suitable for the planned high-temperature operation.

6.2. SELF-CALIBRATE CAPABILITIES

The Phase I "feasibility" system did not include any provision to account for temporal changes in opacity, light source variation, sensor deterioration, or other attenuations of light intensity.

In the system designed for the Phase I testing, a witness diode was incorporated (See Figure 9). The function of this witness is to monitor temporal changes, and correct the measured light intensities.

The assumption is made here that the temporal changes are achromatic, e.q. that a constant factor can be used to account for variations in the measured light intensities, and that the factor is the same for all wavelengths used. While this assumption is satisfactory for changes due to opacity, dust, dirt, thickness variation or surface scratches, it is not entirely satisfactory for variations in the light source voltage, that affects the "color temperature" and therefore the spectral contents of the source.

To evaluate the limitations of the witness efficiency, we conducted a test, using the Phase I system, and changing the lamp voltage within a broad range.

The retardation in a fixed retardation plate (δ = 176 nm) was measured by the SCA system. After the system was calibrated at a nominal lamp voltage of 30 volts, the system was operated at varying lamp voltages.

Table 6 compares the "measured" retardation without witness update and the retardation calculated, including the update.

TABLE VI: CHANGE IN FILAMENT TEMPERATURE

LAMP FILAMENT VOLTAGE	% ATTENTUATION AS SEEN BY WITNESS DIODE	RETARDATION EVALUATED	
		WITHOUT UPDATE	WITH UPDATE
30V	0 *(APPROX.)	180	180
28V	12.5	164	176/180
26V	26	144	172/176
24V	38	128	168
22V	48	112	164/168
20V	60	96.0	160

The results of our evaluation proves that for a lamp voltage 28V ±2 Volts (± 7%), the measured retardation remained within the resolution ability (±4 nm), when corrected by the information collected by the witness.

Clearly, it is possible to maintain the lamp voltage easily within ±2%. The Phase II lamp power supply was regulated to maintain the lamp voltage at 25 V within 0.1%, certainly exceeding the needs and allowing an accurate use of the "witness" concept.

6.2.1. Witness-Operating Algorithm

The diagram below shows the "witness diode" incorporated in the analyzer design. The witness is receiving the light that did not cross

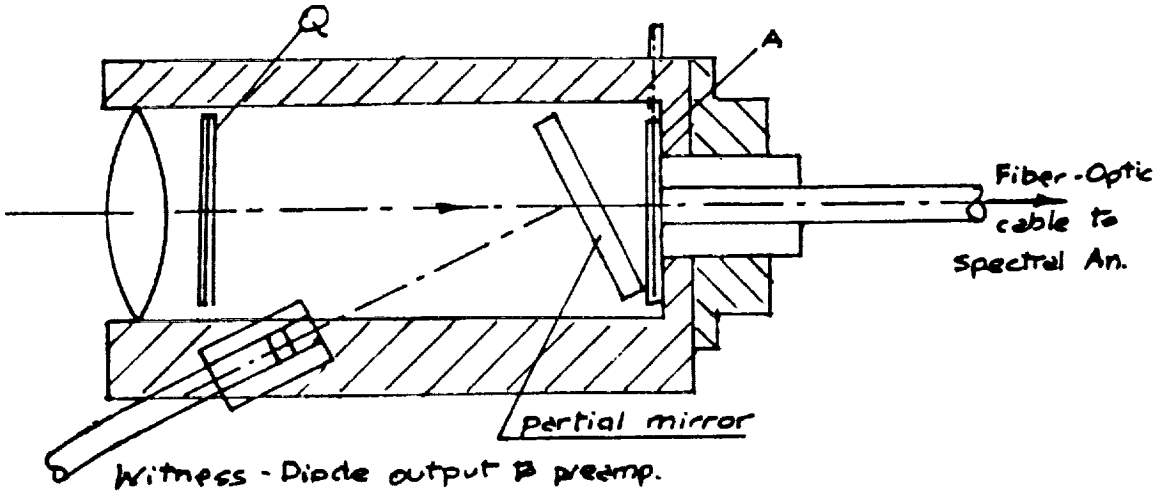

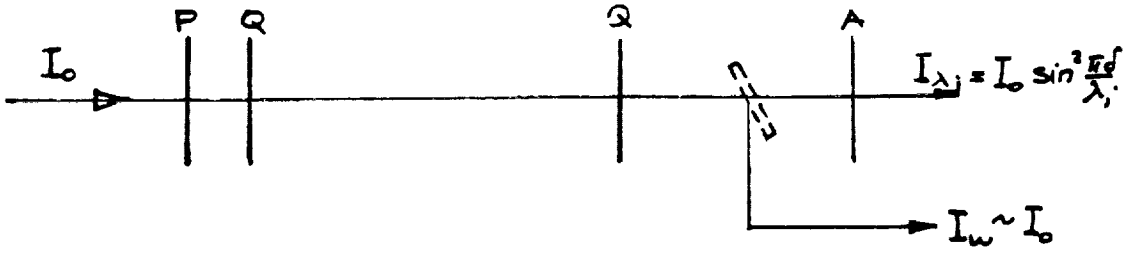

the analyzer, (see figure 9) and therefore is not modulated by the stress term $T_M = \sin^2 \frac{\pi\delta}{\lambda}$.

Referring to the equation (25) that includes the polarizer efficiency "e", we must now incorporate the witness factor W_f, a reflectance of an achromatic partial mirror, diverting a small fraction of light toward the witness diode (approximately 4%).

Since the partial reflector is achromatic, the expression (25) remains the same. An infrared cut-off filter placed in front of the witness insures that the spectral range observed by the witness is the same as the range observed by the array.

During the initial system calibration, the current i (CAL) are recorded in:

LAMP-OFF (NL) -Condition

CALIBRATE (CAL) -Condition, with LIGHT FIELD set up, analyzer parallel to polarizer, not specimen (or a stress-free specimen) within the field of view.

OPERATE (OP) -Condition. Here the instrument is set up in its normal operating position, no specimen (or stress-free specimen) within the field of view.

The currents measured in these three conditions provide all the equation constants and "witness" information, as follows:

Lamp-off

$I_j = D_j$ -Records the dark current of every element of the photodiode array.

$I_w = D_w$ -Records the dark current of the witness.

$I_{jcal} = eI_{o\,j} + I_{o\,j}\,(1 - 3) + D_j$ -Records the overall Spectral calibration $S(\lambda)_j$

$I_{wcal} = I_o \times W_f + D_w$ -Records the witness factor W_f

Operate (CAL)

$I_{j\,OPCAL} = I_o\ (1 - e) = D_j$

$I_{w\,OPCAL}$ (SAME AS ABOVE)

Measure

$I_w = I_{o\,wf}$

Any change in the source I that is achromatic, will introduce a change in the witness output that is used to correct the acquired $I_{o\ j}$ by a factor $I_w/(I_{w_{cal}} - D_w)$.

The system using this correction was implemented and performed in accordance with expectation. In particular, it permitted a broad defocusing range, whereby very large changes in the light intensity received by the array did not affect the calculated retardation.

6.3. MULTI-POINT DATA ACQUISITION SYSTEM

The design of the data acquisition system based on Spectral Contents Analysis (SCA) was the key objective of the Phase II research.

The system was to acquire the light-intensity data from several sensors, located at various locations, transmit this information to a a PC-based data acquisition system and calculate the measured strain, force, pressure, etc.

During the Phase I research, a one-point simplified system was used to demonstrate that it is possible to accurately measure the birefringence using the SCA concept. In the Phase II objectives, the following parameters and design criteria were investigated:

a. Dedicated SCA spectrophotometer

b. Fiber-optic links

c. PC-based data acquisition hardware, for multi-channel measurements

6.3.1. Dedicated Spectrophotometer

The spectrophotometer designed for this purpose included a reflectance diffraction grating, a photodiode array, and a system of lenses providing a collimated light path, focusing the entrance slit on the array.

In the initial Phase I design, 16 photodiodes were used (equally spaced), providing an overabundance of data. In a multichannel system, this large number of photodiodes for each sensor appeared unnecessary, and the research was carried out originally to determine the smallest (minimum) number M of photodiodes required to accurately retrieve the retardation from the equation (12) using the "minimum error" approach (see 3.2 above).

Since sixteen photodiodes were available in the experimental set-up, the test program conducted to minimize the number of photodiodes included the use of:

- Eight equally spaced (20 nm) photodiodes
- Eight photodiodes with increased spacing (40 nm)
- Eight photodiodes with unequal spacing, covering a broad spectrum, but remaining closely spaced in selected spectral bands.
- Twelve photodiodes (20 nm space)
- Sixteen photodioes (20 nm space)

The result of the testing showed that using eight photodiodes:

- The range of the measurable retardation was 4000 nm.
- The closely-spaced arrangement performed better than the broadly-spaced arrangement.
- Variable spacing have increased the range to 4400 nm but requires a complex programming. This is a very promising approach, since it offers a higher speed of operation than the twelve or sixteen photodiode solution.
- The twelve and sixteen photodiode arrangement was performing up to 6000 nm. Above this range (which is in excess of our initial objectives) a smaller spacing of photodiodes will be required. It appears that eight photodiodes or less should be sufficient for most practical applications, where the typical retardation range remains below 2500 nm.

The spectrophotometer photodiode array was mounted on a PC-board that included the preamplifier, converting the photodiode currents into voltage (volt level) shown in Figure 12.

The output from each photodiode was then channeled to the A/D converter using a multiplexer expansion board EXP-16.

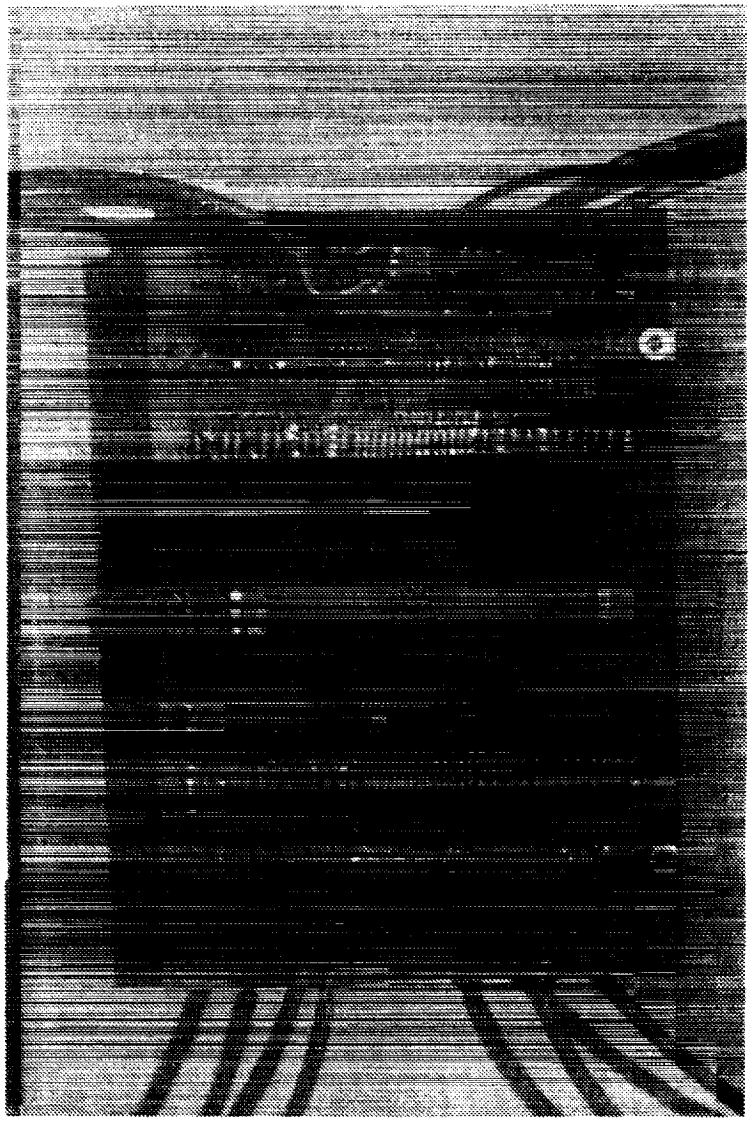

Figure 12. Photodiode Array Mounted on the Preamplifier-PC-Board

The electrical schematic representing the data acquisition system is shown in the Figure 13 below:

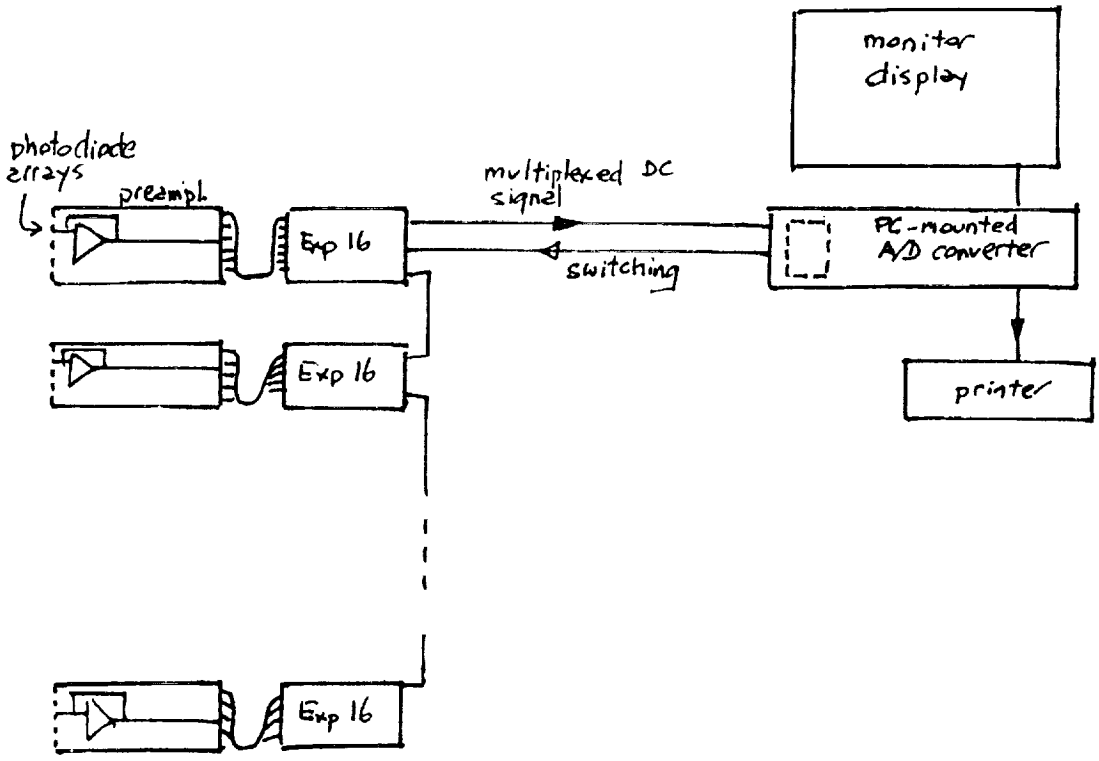

Figure 13. Multipoint Data Acquisition Schematic

Each multiplexer (Metrabyte EXP-16) provides selectable gain and permits scanning of up to sixteen photodiodes of the array. The channels (one to eight) are daisy-chained and interrogated by the computer-housed A/D converter driven by the program.

The individual schematic of the preamplifier board, EXP-16, and the A/D converter are shown on Figures 14, 15, and 16.

BLOCK DIAGRAM

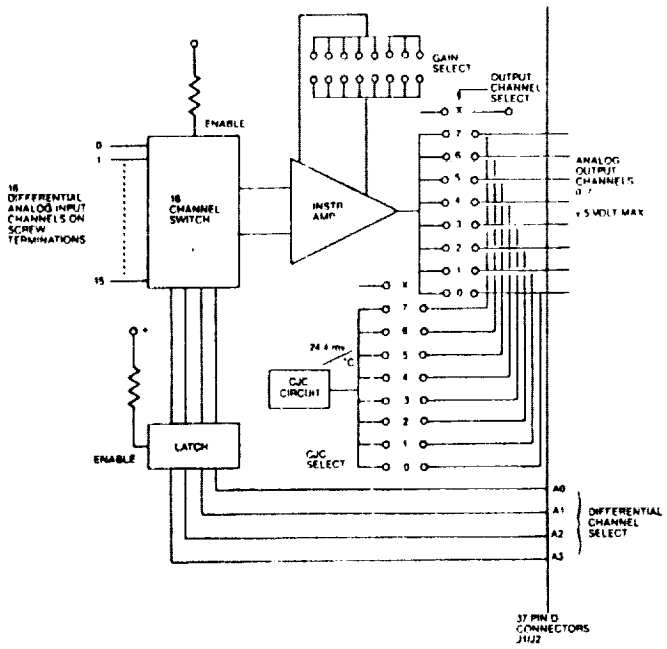

Figure 14. EXP-16 Multiplexer for Data Acquisition from One Array.

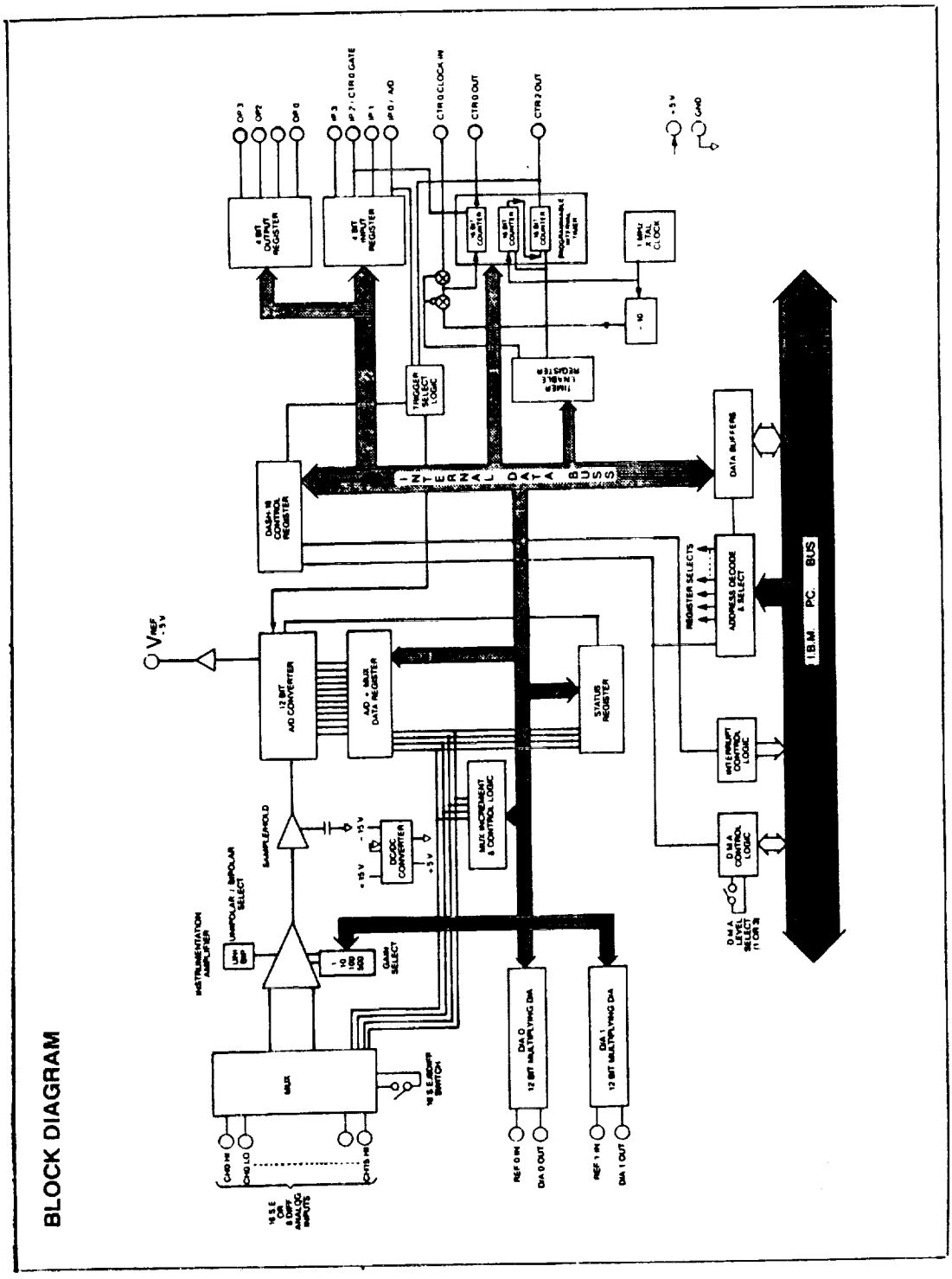

Figure 15. Sixteen-Channel A/D Converter Mounted in IBM XT-PC for Data Acquisition.

39

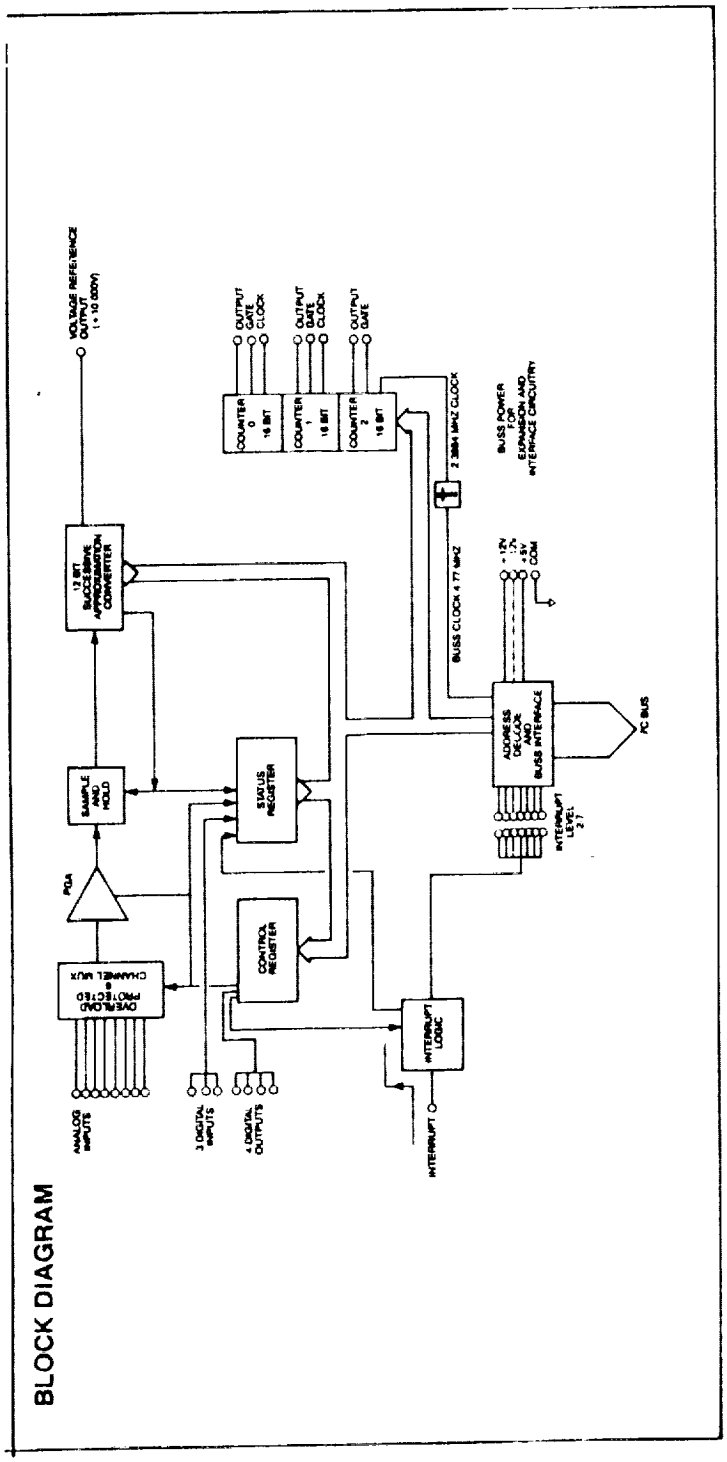

Figure 16. Eight-channel A/D Converter, Capable of Handling Up to Eight Boards EXP-16.

40

The system was tested extensively, without any problems.

The speed of data acquisition (at 100,000/sec. conversion rate of the A/D converter), using as example four channels and eight diodes per channel is approximately 3000 per sec. The speed of data acquisition is higher than the speed of data reduction, and falls in the class of "quasi-dynamic" acquisition.

6.4. DYNAMIC DATA ACQUISITION FOR SPECTRAL CONTENTS ANALYSIS METHOD

The project of analysis, software development, evaluation, and experimental verification was subcontracted with Lehigh University. The work was completed in February-March 1989 and encompassed the testing of a system shown schematically below:

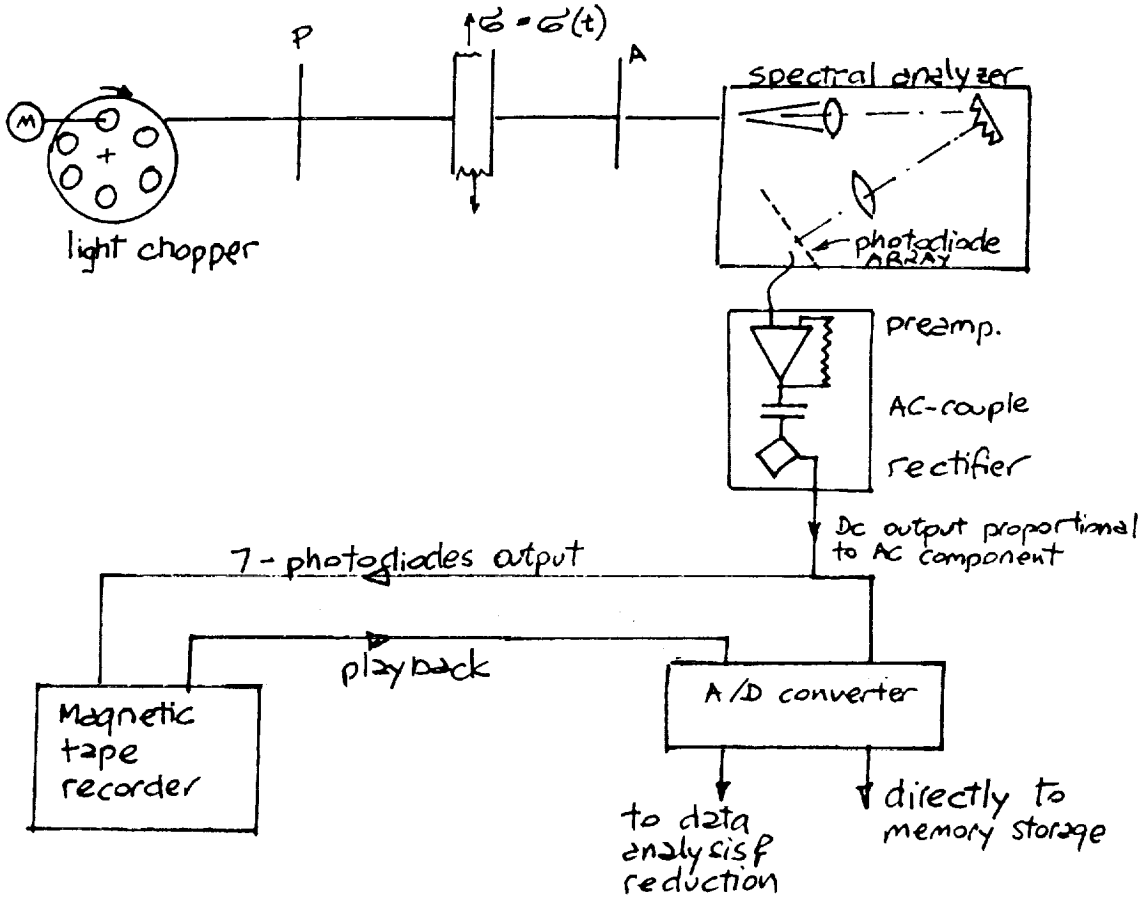

Figure 17. Schematic of Dynamic Data Acquisition

6.4.1 Analysis

The Spectral Contents Analysis system is based on the analog data acquisition by a set of photodiodes. The dynamic speed of response of these diodes is much higher than any other component in the data acquisition and analysis system. To measure birefringence at a point, the signals obtained from at least seven photodiodes are amplified and have to be stored simultaneously. In the current set up, which was designed for static and quasi-dynamic data acquisition, the data is acquired at the maximum multiplexer speed from all photodiodes and averaged 64 times, (to eliminate noise). After that step, all necessary calculations are performed to get the desired retardation at a given point and the whole process is repeated again. It takes about 1.5 seconds to complete this process. Thus, in the present configuration only slowly varying signals can be evaluated, with frequency below 1/3 Hz.

Two possible methods can be implemented for the acquisition and analysis of fast changing signals. The first one is a direct connection of the amplifiers' output to an analog-to-digital converter capable to accept eight channels of data. The Metrabyte DAS-16 A/D converter implemented in the current system, has a stated throughput of 50,000 conversions per second, (Note that the faster A/D converters are presently available). Assuming data acquisition at eight channels, one can get 6,250 scans per second. At such a rate the CPU memory will be exhausted after approximately 640 msec. However, such data acquisition speed will be able to record signals with frequency components up to 3,125 Hz, which is rather high. Assuming the necessity to acquire signals with frequency not exceeding 100 Hz, one will be able to acquire data for 20 sec. without transferring the information to the hard disk. For longer times of data acquisition, one has to sacrifice frequency resolution to increase the recording time. For long data acquisition times (order of minutes and above) one may be able to acquire data and store it on the hard disk, however such a process is rather time consuming and cannot be used with reasonable fast varying signals. Thus, the direct use of the A/D converter to record dynamic data is limited to fast varying signals (over 1000 Hz) and short data acquisition times (order of one second) or lower frequencies and correspondingly longer times of the recorded signals.

Presently available A/D high speed interface with on-board memory (Metrabyte Model DAS-50) can acquire four channels at 1,000,000 samples per second and store them on the 1 Megaword memory buffer on-board. One can use two such boards for analysis of the events of up to one second duration with frequency components up to 125 kHz.

The second alternative approach may be implemented for investigation of the signals having frequency components up to 1250 Hz but requiring the recording time which may exceed the capability of the CPU memory. For these applications, a magnetic tape recorder should provide the answer. For example, the TEAC MR-30 portable cassette data recorder used in evaluation testing is able to record seven channels of data with frequency response DC to 10 kHz for as long as 5.6 minutes without changing signals, i.e. DC-1250 Hz, up to 45 minutes of data can be stored on one cassette, while for DC-313 Hz up to 180 minutes of data can be recorded. The recorded data can be played back later into the Metrabyte A/D converter at a proper speed and evaluated as described above.

6.4.2. Experimental Verification

To evaluate the capability of the existing system to acquire and process dynamic data, an experiment was performed. The software was developed to acquire data from eight photodiodes at the fastest possible rate. This information was kept in the computer's memory; after memory capability of the existing system was exhausted, the stored information was processed, using the SCA algorithms and extracting the retardation from the acquired light intensity.

In the present set up, it takes 0.380 milliseconds to scan all eight channels, resulting in 2.6 kHz sampling rate. Only 1000 scans can be acquired before the "memory full" message appears. However, we did not try to optimize the software. Currently available computers can accommodate much larger arrays (i.e. MS FORTRAN ver. 4.1 with HUGE memory).

In order to evaluate the influence of the system noise on the calculated retardation, we used a specimen with "frozen" birefringence. Utilizing our standard procedure, which acquires 64 scans, averages them and then uses this informtion to calculate retardation, value of 772 nm was obtained. To simulate dynamic data acquisition, data was acquired for the same specimen. Sixty-four scans were acquired, however, each one was processed separately. The obtained retardations show very good performance of the dynamic system. The average measured retardation was 772.38 with the standard deviation of 2.83 for 64 scans. These results confirmed that the suggested approach for dynamic data acquisition is a valid and accurate way to measure birefringence during dynamic events.

From the analysis of the obtained data, one may conclude that the spectral contents analysis is capable to analyze the dynamic events. Direct utilization of the SCA with the DAS-16 A/D converter resulted in sampling rate of 2.6 kHz, while there is

a possibility to use more advanced hardware and increase the sampling rate for eight channels up to 125 kHz. When there is a need for longer times of data acquisition, one may use analog FM tape recorders for data acquisition, with consequent playback into A/D board and processing by computer.

The described dynamic Spectral Contents Analysis system can be used in a variety of industrial and laboratory applications, where there is a need for fast, automated data acquisition, processing, and analysis.

6.5. DATA ACQUISITION USING SINGLE FIBER FOR DATA TRANSMISSION

One of the important advantages of the birefringent sensor is the stability of the sensor materials. In civil-engineering applications, embedded sensors are frequently used for remote sensor of stresses in rocks (mines, seismology) and in concrete (bridges, pilons, footings).

In these applications, long-term stability is essential, and noise-free data transmission of fiber-optic cables offers a significant advantage.

The Spectral Contents analysis method can be used for data acquisition from these embedded sensors using long fiber-optic cables, available at a reasonable cost in a form normally produced for communications industry. The large diameter, single-fiber cables, 280 microns in diameter (.008 in.), is available for use with standard fiber-optic connectors (AMP 905).

The light-intensity losses occur primarily at the entrance and at the connector. The objective of this investigation was to assess if the transmitted light intensity is sufficient for data analysis and retrieval of the retardation from the light transmitted by the birefringent sensor. The cable assembly including a standard 200-micron diameter clad cable with a jacket and type 905/906 SMA connector at each end was procured from Aurora Optics, Blue Bell, PA. The cable was connected to the analyzer head and to the spectrophotometer box on the other end, replacing the 1/16 diameter bundle used in the system.

The currents i_j measured by the spectrophotometer were approximately four to five times lower than the currents i_j measured using the 1/16 diameter bundle used in all previous testing.

The signal (volts) measured after the preamplifier was 300_m V. Since the system noise was typically below 3_m V, (1% of the signal) it was concluded that the single-fiber data transmission can be used effectively, provided the diameter of the fiber-optic cable remains sufficient to carry the required light intensity.

7. SOFTWARE DESCRIPTION

The unknown retardation can be evaluated on the basis of equation (12) as described in the section 3.1. The computer program doing this can be described as following:

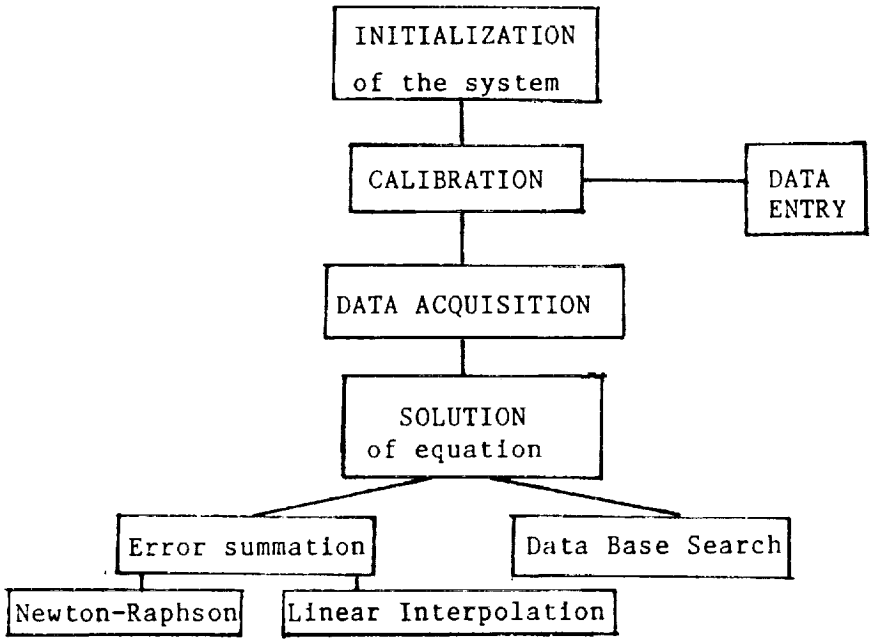

7.1. INITIALIZATION OF THE SYSTEM

The first part of the program assigns all necessary arrays to be used in the process of evaluation of the retardation.

- DI(512,16) - contains theoretical transmittance for each one of the 512 values of retardation within the selected range (0-5120 in 10 nm increments) for every one of the 16 available photodiodes.

- DM(16) - contains actual readings for a given retardation at each one of the 16 photodiodes.

- DC(16) - contains dispersion coefficients for a given material at each one of 16 photodiodes.

- BF(16) - contains actual readings for an un-stressed specimen in the light field set-up for each one of 16 photodiodes.

- DF(16) - contains actual readings for an un-stressed specimen in the dark-field set-up for each one of 16 photodiodes.

- E(512) - values of the error function as calculated in the error-summation part.

7.2. CALIBRATION

At this point of the procedure an unstressed specimen is installed in the light field circular polariscope set up and the transmitted light intensity is acquired into array BF(16). The set up is then changed into the dark field arrangement and corresponding values of light intensity are acquired into array DF(16). This information is then used to calculate proper values for I (j). The operator enters from the keyboard the thickness of the specimen and physical constants required for computation of the stresses.

7.3. DATA ACQUISITION

The A/D converter supplied by METRABYTE was used to acquire DC-voltage proportional to the light intensity and convert them in the digital form. Each photodiodes output is sampled 64 times and the average value is used in the evaluation procedure. The total time to sample 64 times each photodiode to convert its output in the digital form and find average values, takes less than 1 second for all 16 photodiodes.

7.4. SOLUTION

7.4.1 Error Summation

This part of the program calculates theoretical values DI(512, 16) of light intensity observed by each photodiode at each specified retardation according to equation (10) and compares it to the acquired data as described in section 3.2.

7.4.2. Newton-Raphson

The function g(i), is formed according to 3.2, all necessary derivatives are calculated and a linear system of equations is solved for a given set of initial values of the unknowns. The solution is used as an input value for the next iteration. This process is repeated until necessary convergence is achieved.

7.4.3. Linear Interpolation

To increase the resolution of the results in the "error summation" approach, a simple technique of linear interpolation is used. The interval of wavelengths observed by each photodiode is divided into smaller (subdivisions 8.3. 1 nm) and process of error summation is repeated for this range.

7.5. "WITNESS CORRECTION" PROCEDURE

Since the light intensity does not remain constant, a "self-calibrating" system was incorporated. Let us introduce a witness diode, which is reading unpolarized light as it enters the analyzer probe.

The total light intensity acquired by each photodiode can be represented as follows:

$$I_i(\delta) = \int_{\lambda_{i_1}}^{\lambda_{i_2}} I_{o_i}(\lambda)\sin^2\left(\frac{\pi\delta}{\lambda}\right) * (1-0.5 * \sin^2 e_q)\, d\lambda + DF(i) + NL(i)$$

where DF(i) - represents light intensity as recorded by i-th diode due to the polarizer,

NL(i) - is light intensity recorded by i-th diode, when light source is off

λ_{i_1}, λ_{i_2} - represent the lower and upper boundaries of the spectrum acquired by a photodiode "i".

Each term in the equation (A1) will be modified proportionally to change in the light source output. Assume, that the witness diode is reading value of W(i), thus the equation (A1) can be modified as follows:

$$I_i(\delta) = \frac{W(i)}{D\,F(i)} \cdot \int_{\lambda_{i_1}}^{\lambda_{i_2}} I_{o_i}(\lambda)\sin^2\left(\frac{\pi\delta}{\lambda}\right) * (1-0.5 * \sin^2 e_q)\, d\lambda + DF(i) \cdot \frac{W(i)}{D\,F(i)} + NL(i)$$

where W(i) is the witness diode reading.

This approach was incorporated in the Version 2 of the developed software and was built in the multi-channel spectral contents analysis system. This term is now an input into the SOLVE routine. Using this version, one does not have to calibrate the system each time it is turned on. The program saves the results of calibration and gives the user a choice of performing a new calibration or possibility to use the previous one.

8. DATA ACQUISITION AT 2000° F

The use of a birefringent sensor and the data acquisition at elevated temperature was one of the important objectives of this program. To accomplish this objective, the following elements needed to be developed are:

a. Sensor capable of operation at elevated temperature.
b. Optical link between the sensor and the readout system.
c. Data analysis capable of differentiating between the strain, and changes in temperature.

All above problems were investigated and resolved.

8.1. SENSOR FOR ELEVATED TEMPERATURE

The research on sensor materials (see section 5, "Sensor Material and Geometry) led to the selection of FUSED SILICA as the best candidate material. The calibration of fused silica was performed at room temperature on a ½" x 1" x 6" specimen subjected to uniaxial compression. The Brewster constant was found to be $C = 3.4 \times 10^{-12}$ m²/N.

The calibration at elevated temperatures was performed in a high-temperature test chamber, on a disc subjected to diametrical compression. The force was carried by a stainless-steel lever system and measured by a load cell placed outside of the oven.

The fringe order was measured visually using a senarmontite compensator at temperatures ranging from room temperature up to 1100° C.

The photo figures 18 and 19 show the experimental set-up, the specimen installed inside the oven and the lever system used.

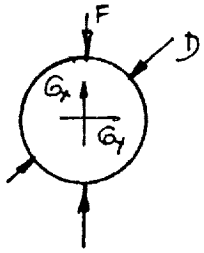

For a disc subjected to a diametrical compression, the stresses at the center are:

$$\sigma_x - \sigma_y = \frac{8F}{\pi Dt}$$

and the retardation measured at the center is:

$$\delta = C_B (\sigma_x - \sigma_y) \times t = \frac{8F}{\pi D} C_B$$

yielding:

$$C_B = \frac{\delta}{F} \frac{\pi D}{8}$$

where C_B is the Brewster constant

δ is the measured retardation

D is the diameter

F is the applied force

The graph figure 20 shows δ vs. F at various temperature levels. This figure clearly demonstrates that:

a. The Brewster constant remains constant between room and 1100° C.

b. The measured birefringence yields the stress and is independent of the temperature.

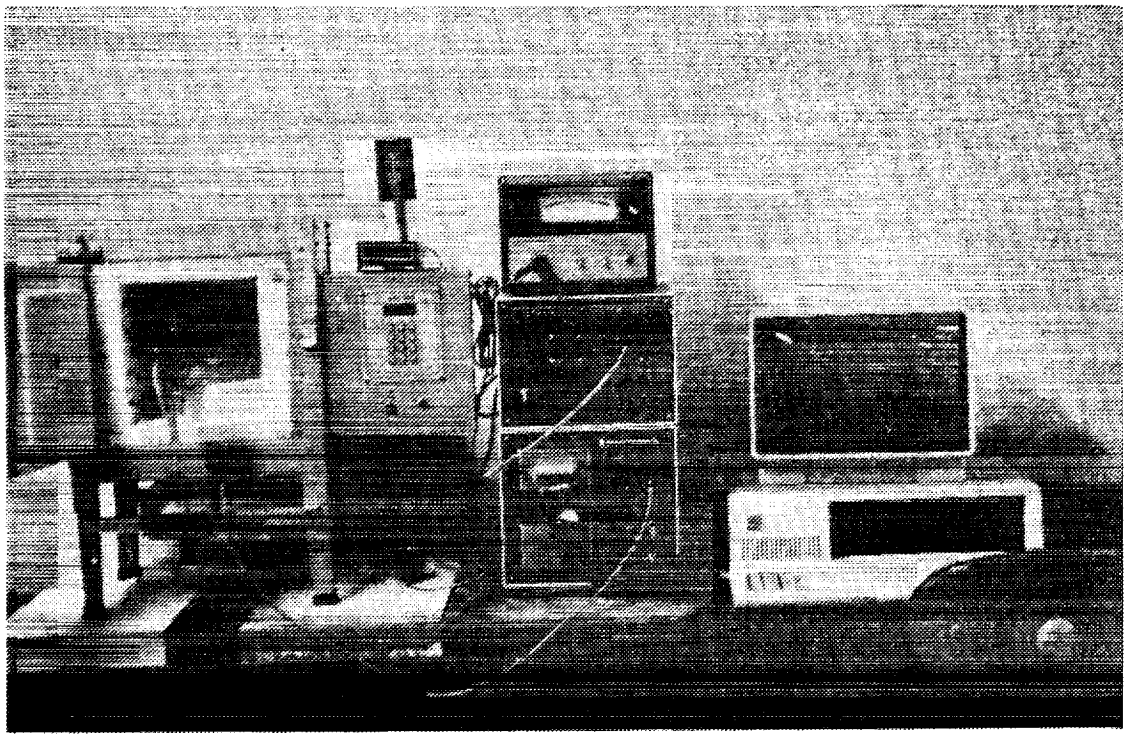

Figure 18. Experimental Set-Up for Measurements of Birefringence at Elevated Temperatures using the SCA System.

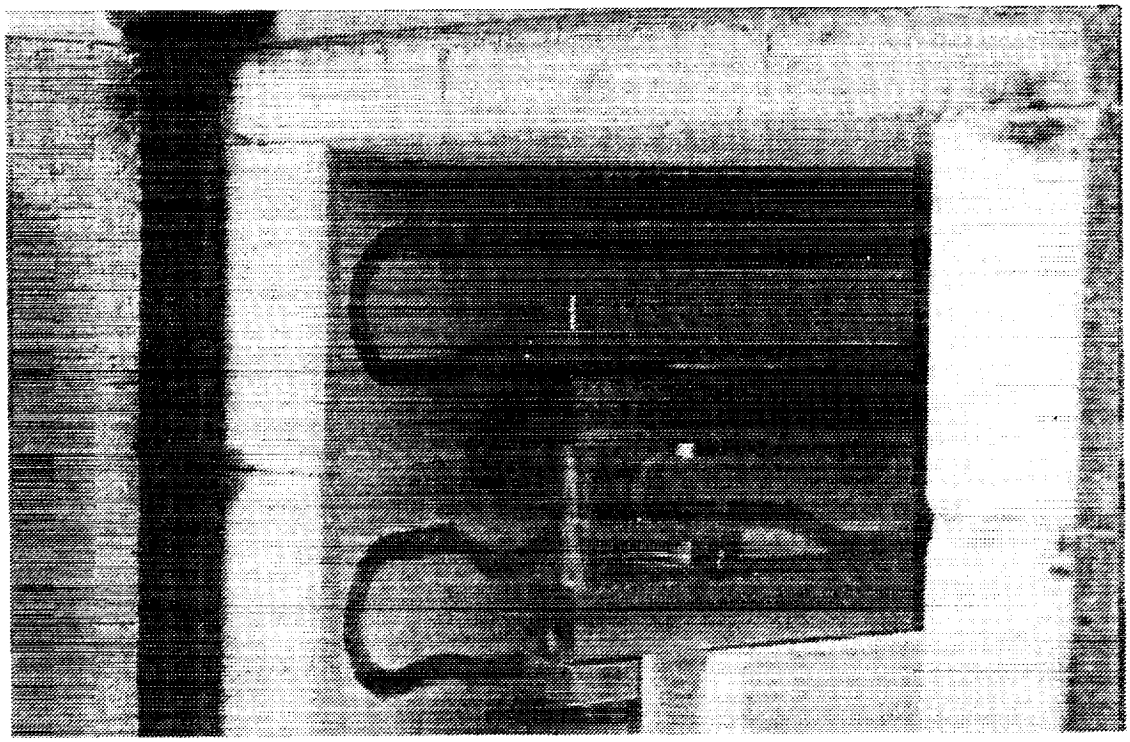

Figure 19. Fused Silica Disc Subjected to Stress using Dead Weights and Levers.

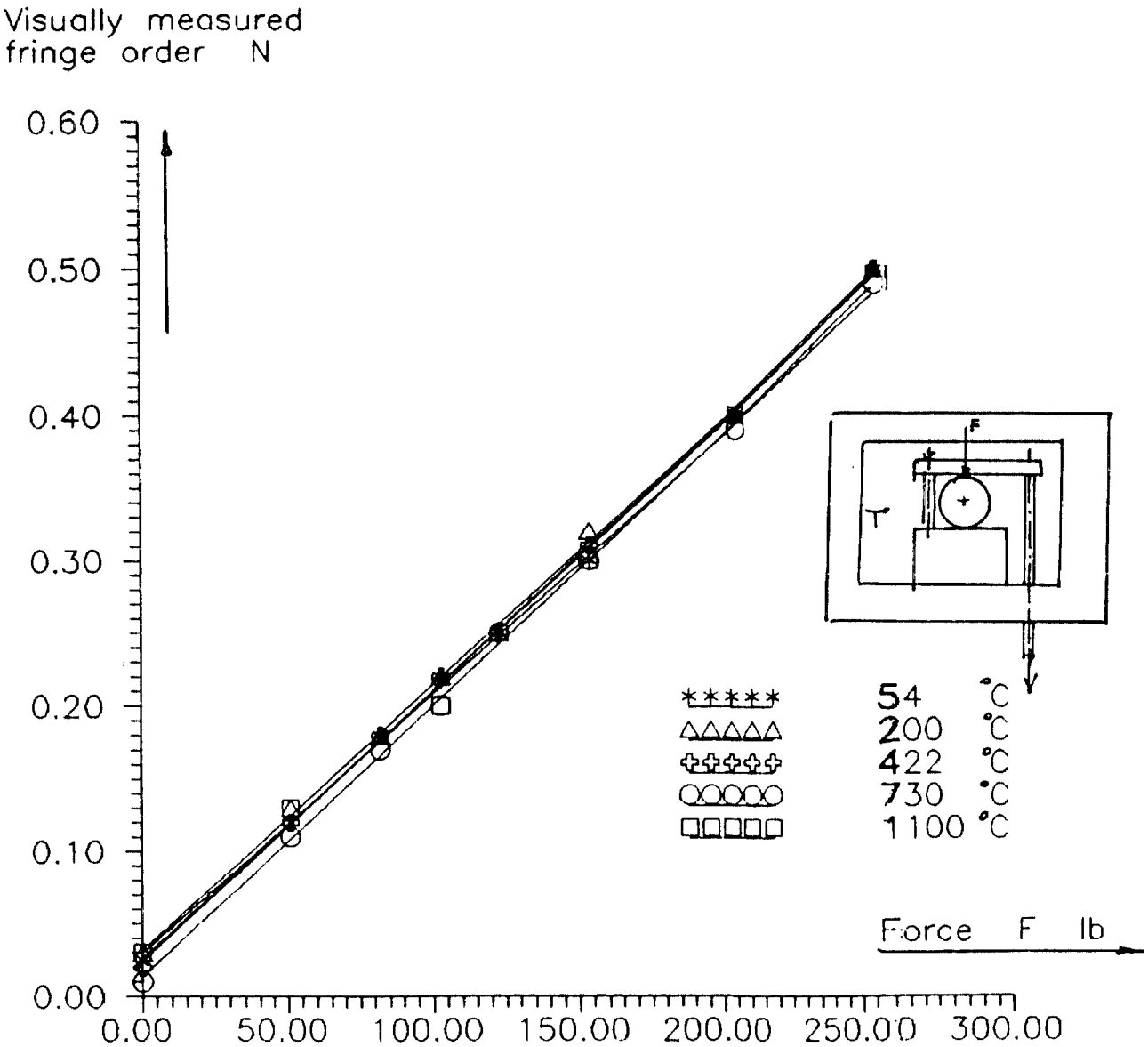

FIG. 20. EVALUATION OF STRESS-OPTIC RESPONSE OF FUSED SILICA VS. TEMPERATURE.

8.2. OPTICAL LINK AND ACCESS METHODS

In the course of the research, several approaches were investigated and evaluated, for data acquisition at elevated temperature (See 6.1 above).

a. Probes Located Outside and Using Only an Optical Link

This approach is the simplest and most accurate, since no part of the optical system is exposed to elevated temperature.

Only a fused-silica window is required to provide a line-of-site access to the sensor. Such a window is an easily available commercial item available from every supplier of optics component.

We used this approach to collect the data from the specimen located inside the oven, measuring the stress in the disc used for calibration purposes.

The result of these measurements are shown in Figure 21 . These results are in perfect agreement with the senarmont method and demonstrate the accuracy of the system.

b. Penetrator

A "penetrator" (see Figure 10) was designed to provide an optical link to a sensor that is not accessible to a direct line of site.

In this design, the polarizer elements are exposed to elevated temperature. This design was evaluated and the energy efficiency of polarizers was not very high (see Figure 11 and table).

The "penetrator" is relatively expensive and must be custom-designed for each application. Some elements (stack of plates, lenses, ...) are common for a large variety of applications, but the tubular members made of refractory materials are not generally reusable.

This solution is not ideal and should be considered only when other approaches fail.

c. Fiber-Optic Links

The feasibility of "single-fiber" link was demonstrated and tested.

Presently, several manufactures offer "polarization-preserving" fiber-optic guides. While not available commercially at this time, a fused-silica polarization-preserving fiber-optic cable will become within the near future an ideal link to a fused-silica sensor.

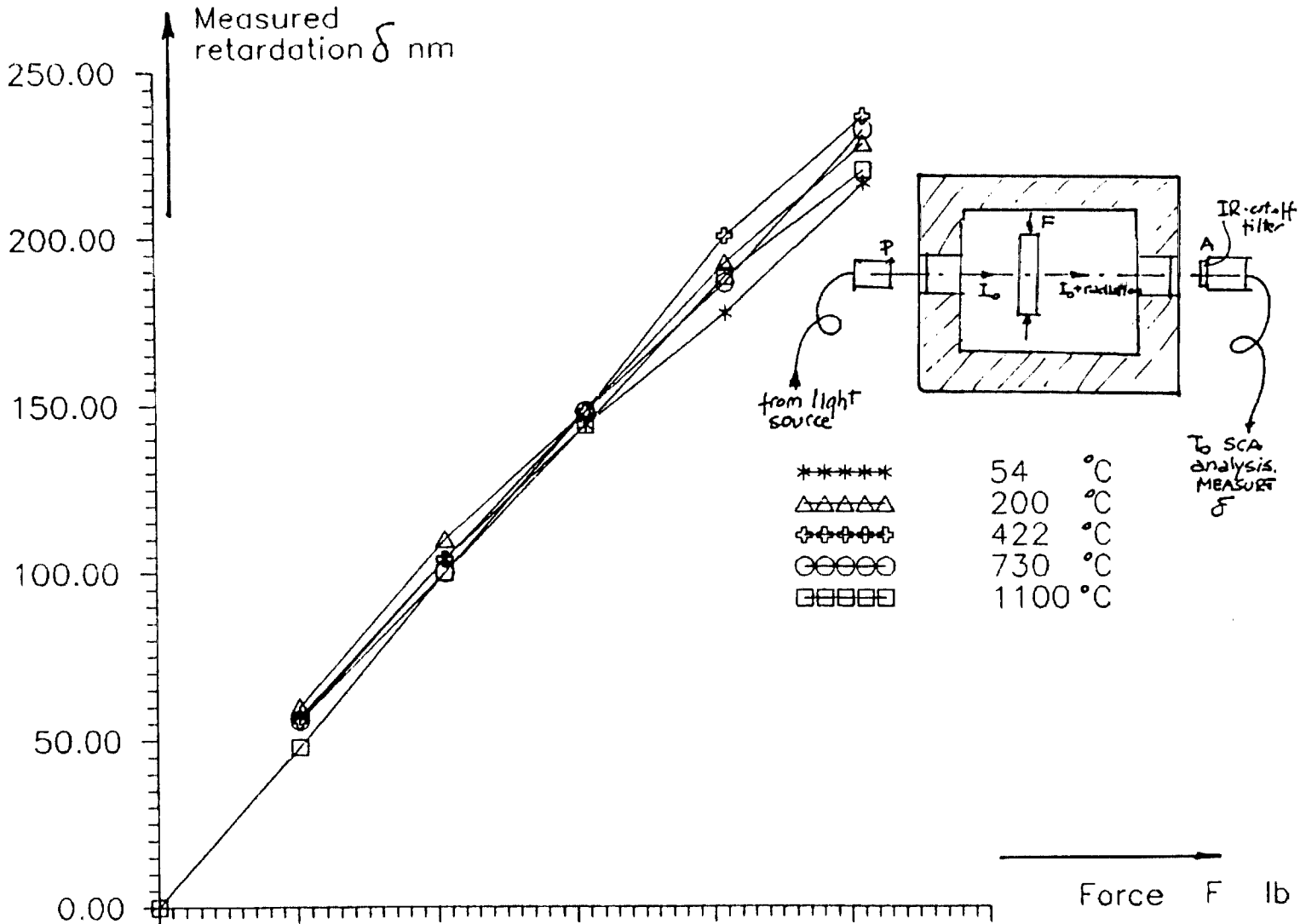

FIG. 21. SYSTEM EVALUATION. MEASUREMENTS OF RETARDATION IN FUSED SILICA IN TEMPERATURE RANGE 54C TO 1100 C

8.3. SIGNAL PROCESSING - DATA ANALYSIS

At elevated temperature, the sensor itself radiates energy and a portion of this energy is included within the spectral range used in the data acquisition. During the research and design of the data acquisition, two systems were developed and tested to eliminate the specimen-radiation effects.

8.3.1. Optical Filtering

Most of the radiation energy (Wien Law) up to 1100° C is emitted at wavelengths above 1 micron, and only a small portion is contained within the range of wavelengths used in our spectrophotometer. To eliminate the specimen radiation, a cut-off (low-pass) filter was used to cut-off radiation above 800 nm.

This approach proved very effective, when combined with frequent calibration of the system to account for unpolarized light.

8.3.2. Electronic Filtering

The electronic filtering is also possible, and is certainly advantageous for temperatures in excess of 1000° C. The electronic filtering includes:

a. A "Chopped" Light Source

The chopped light source can be simply produced by mechanical obstruction (spoked wheel) of the light source. We have introduced a wheel containing eight holes and spinning at 30 Hz generating a 240 Hz "carrier" frequency of the source.

b. An "AC" Pre-amplifier for the Photodiode Array

A multi-channel preamplifier was designed, including a capacitor at the preamplifier output, filtering out the "DC" energy (due to specimen radiation) and transmitting the AC component of the light-source carrier frequency. The schematic of the circuit is shown in Figure 22 .

The combination of the "chopped light source" and "AC" preamplifier was tested and found satisfactory. This system is not essential for operation at 1000° C and below, but becomes necessary for operation of the SCA system at higher temperature and for future expansion to even higher temperatures.

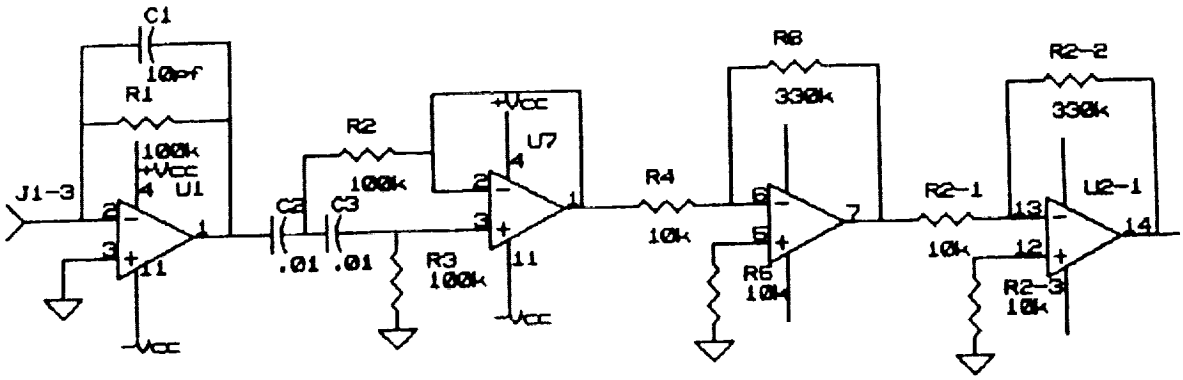

AC Preamplifier Tuned to the Chopper Frequency, and Rejecting the DC (radiation) Energy.

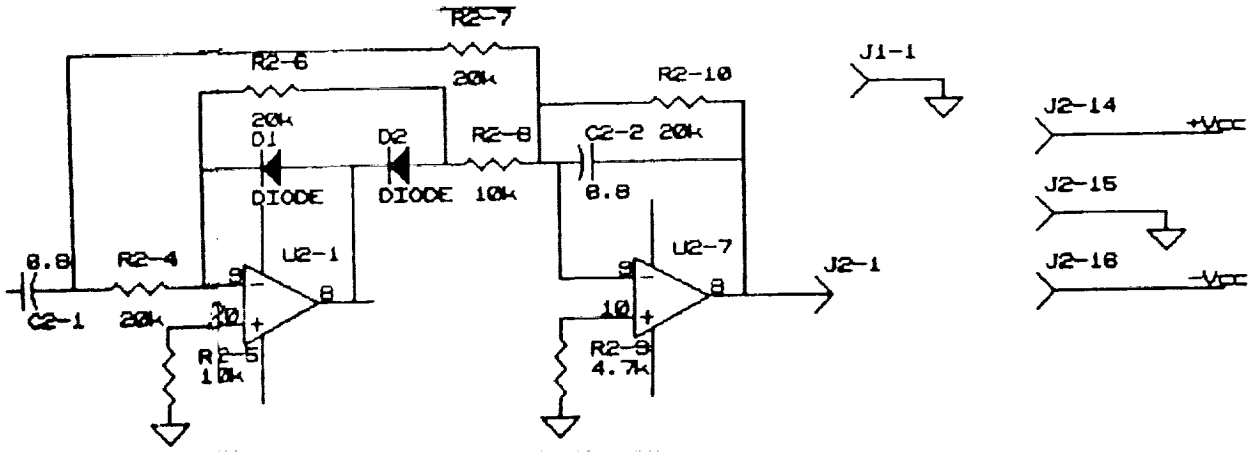

Rectifier Yielding 2-DC Output Connected to EXP-16 Multiplexer

Figure 22. AC Preamplifier, Rejecting the Specimen Radiation Component

8.4. PRECISION OF STRESS MEASUREMENTS AT ELEVATED TEMPERATURE

There is no reference method that can be used for evaluation of measurements that were performed at 2000° F. From Figure 18 it can be stated that the scatter of the data points and the departure from the straight-line was approximately 10 to 20 nm representing only 1 percent of the practical range covered by the system. Some of the scatter was due to the friction in the lever system and imperfection in the surfaces contacting the evaluation specimen. However, even if all of the scatter is attributed to the SPECTRAL CONTENTS METHOD, this precision exceeds all presently available methods.

9. CONCLUSIONS

As a result of the research, engineering and development work sponsored and funded by the Phase I and Phase II programs, all the research objectives were met, and in many instances exceeded, in particular:

a. The feasibility of the Spectral Contents Analysis method of measuring birefringence was demonstrated (Phase I).

b. A data acquisition system capable of measuring strain using bonded or unbonded birefringent sensors was designed, constructed, tested, and evaluated.

   Similarly to an electrical resistance sensor data acquisition, the system permits:

   - Multipoint Data Acquisition
   - Dynamic Data Acquisition
   - Data Acquisition at Elevated Temperature

   The system permits data acquisition from remote location using a fiber-optic cable, immune to the EM & RFI.

c. Several significant engineering innovations were made, and a technology previously unavailable is now available, in particular:

   - Remote acquisition of birefringence data using fiber-optic cable is routinely made using the SCA system at room and elevated temperature.
   - Measurements of retardation at 2000° F were made possible.
   - Brewster Constant of fused silica at 2000° F was measured accurately, permitting quantitative stress measurements using fused silica as a sensor.

10. PHASE III - COMMERCIAL APPLICATION

In the Phase II proposal STRAINOPTIC TECHNOLOGIES expressed commitment to continue the R&D work, and develop a commercial system, based on the principles of the Spectral Contents Analysis.

Since the research work described above was concluded and a measuring system was designed, STRAINOPTIC is now preparing a commercial system for measuring birefringence to be used for the following applications:

- Measuring of strain-birefringence in oriented-film production (2) (polymer-industries, film production).
- Measuring of strain-birefringence in float-glass production.
- Dedicated sensors for long-term, remote-data acquisition (embedment gages)for civil-engineering structures.

A commitment was also expressed by MEASUREMENTS GROUP of Raleigh, North Carolina contingent on the successful completion of the Phase II. STRAINOPTIC will approach the MEASUREMENTS GROUP to inquire about their interest in the development of an instrument for data acquisition from photoelastic coating.

APPENDIX I

LIST OF SYMBOLS

C	- Speed of light in vacuum
v	- Speed of light in transparent media
n_1 n_{x_1} n_y	- Index of refraction
ε_1 ε_x ε_y	- Strains
σ_1 σ_x σ_y	- Stresses
C_B	- Brewster constant
K	- Strain-optic constant
t	- Thickness of material
δ	- Retardation (relative)
β, α	- Direction of principal stresses
I, I_j	- Light intensity, current output
a	- Amplitude
λ	- Wavelength of light
T	- Transmittance
i, i_j	- Photodiode current
S	- Spectral calibration constant
E	- Error function
η_{eff}	- Efficiency of polarizer
F	- Force
D	- Diameter

APPLICATION PROCEDURES

CERAMABOND™ 503, 552, 569, 571 AND ULTRA-TEMP™ 516

A) Surface preparation and application:

1) All surfaces to be bonded or coated should be free of dirt, grease, or oil. If possible roughen surfaces. Prior to bonding, the mating parts should be washed in a strong water base detergent, rinsed and dried. Some porous materials will absorb the liquid binders (wick up). Moistening the surface with water is recommended to prevent this.

2) The clearance between mating parts should be kept uniform and held between .001" and .010". A uniform glue line held in this range is essential to good adhesion. Pressure should be applied and maintained until drying is complete. Avoid repeated squeezing which causes air to be drawn into glue line, and this weakens the bond.

3) The adhesive should be mixed thoroughly just prior to use. Avoid excessive stirring which will entrap air and soften the joint. 571 is the only two component product in this group. Mix at a ratio of 1 part liquid to 1.5 parts powder by weight. Store all these materials at room temperature in a closed container. Refrigeration will not extend the shelf life and freezing could damage them.

4) Apply the adhesive to the surfaces to be bonded in a thin coat using a spatula, brush, spray or dispenser. (See Aremco Dispens-A-Matic™ 7300 product bulletin.) Wetting the surfaces by agitating the bond layer will aid in the strength of the joint.

5) Immediately press the surfaces together maintaining a uniform glue line by fixturing if necessary. Wipe away excess before drying.

6) Note: it is preferable to cure all these adhesives to develop maximum properties. However, if no heat cure is possible in your application, you should use Ceramabond 569 or 571.

B) Curing Schedule :

Products 503, 516, 552 a heat cure is required. Products 569 and 571 it is recommended but not required. Follow the schedule below if possible.

1) Air Set from 1 to 4 hours.

The setting time is dependent on the following factors, the size of area of the glue line (sq. in.) and the porosity of the materials being bonded. The purpose is to remove liquid moisture gradually to increase the density of the adhesive.

2) Oven Drying, 200°F (93°C) for 2 hours.

Oven drying is dependent on the areas and porosity as well. If possible a longer time period should be used to assure complete elimination of free moisture prior to a heat cure schedule.

3) **Heat Cure, 250°F (121°C) for 1 hour.**

The heat cure drives away the waters in the supersaturated liquid binders. Once again longer periods may be used.

4) **Firing Procedure, 250°F (121°C) to 700°F (371°C) one hour.**

This will develop maximum adhesion and moisture resistance on all products. Note: This is a necessity for 503 to maintain integrity in humid environments.

C) Coating Procedure :

503, 552, 569, 571 Thin with potable water up to 5% by volume. Ask for the specific chemical thinner, if a larger dilution is required for products. Spray in thin coats, air dry and re-spray. Cure per instructions in Section B. 516 thin with Ceramacoat 512-T thinner as required. Spray in thin coats, air dry and re-spray. Cure as above.

D) Bonding porous surfaces :

Special care must be used to prevent the liquid binder from soaking into surface.

1) Moisten surface with water. Do not have liquid droplets present to dilute adhesive.

2) Bond pieces together: Refer to general instructions part A.

3) Air set for a longer period of time to allow additional water to escape gradually.

4) Cure (refer to section B.)

E) Bonding materials with dissimilar Coefficient of Thermal Expansion :

If materials have gross differences in CTE, then a graded adhesive line should be formed. Take the best recommended adhesive for each surface and coat them. Allow these coatings to air set. Take a third adhesive with a CTE between both and bond the two coated surfaces.

i.e. Nickel coat with 571, Alumina coat with 503, Bond with 552.

F) Safety precautions :

1) Prolonged skin contact should be avoided due to possible irritation.

2) All products can be washed from skin with a mild soap and water in the uncured state.

3) If any material contacts eyes, flush continuously with water or neutralizing solution; then consult physician immediately.

BIBLIOGRAPHY ON SPECTRAL CONTENTS ANALYSIS METHOD

(REFERENCES)

1. Redner, A.S. "Photoelastic Measurements by Means of Computer-Assisted Spectral Contents Analysis", Proceedings of the 5th Internation Congress on Experimental Mechanics, Montreal, Canada, 1984, pp.421-427.

2. "Photoelastic Measurements of Residual Stresses for NDE", Proceedings, SPIE, 814(1), 1987, pp. 16-19.

3. Sanford, R.J. "On the Range and Accuracy of Spectrally Scanned White Light Photoelasticity", Proceedings 1986 Spring Conference on Experimental Mechanics, New Orleans, LA, 1986, pp. 901-908.

4. Pindera, J.T. and G. Cloud. "On Dispersion of Birefringence of Photoelastic Materials", Experimental Mechanics, 6(9), pp. 470-480, 1966.

5. Zandman, Redner, and Dally. "Photoelastic Coating", SESA, Mongraph #3, Iowa Press, 1977.

NASA National Aeronautics and Space Administration

Report Documentation Page

1. Report No.	2. Government Accession No.	3. Recipient's Catalog No.
NASA CR-179444		

4. Title and Subtitle	5. Report Date
SPECTRAL CONTENTS READOUT OF BIREFRINGENT SENSOR	October 1989
	6. Performing Organization Code

7. Author(s)	8. Performing Organization Report No.
Alex S. Redner, P.I. President	H-1581 / #87-955
	10. Work Unit No. RTOP 505-63

9. Performing Organization Name and Address	11. Contract or Grant No.
STRAINOPTIC TECHNOLOGIES, INC. 108 West Montgomery Avenue North Wales, PA 19454	NAS2-12666
	13. Type of Report and Period Covered FINAL REPORT Period 7-13-87 to 7-13-89

12. Sponsoring Agency Name and Address	14. Sponsoring Agency Code
NASA-Ames Research Center Dryden Flight Research Facility P.O. Box 273, Edwards, CA 93523-5000	NASA

15. Supplementary Notes

NASA Technical Monitor: V. Michael DeAngelis, Ames Research Center, Dryden Flight Research Facility, Edwards, California 93523-5000

16. Abstract

The technical objective of the research program reported here was to develop a birefringent sensor, capable of measuring strain/stress up to 2000° F and a readout system based on SPECTRAL CONTENTS ANALYSIS. As a result of the research work, a data acquisition system was developed, capable of measuring strain birefringence in a sensor at 2000° F, with multi-point static and dynamic capabilities.

The system is using a dedicated spectral analyzer for evaluation of stress-birefringence and a PC-based readout. Several sensor methods were evaluated. Fused silica was found most satisfactory. In the final evaluation, measurements were performed up to 2000° F and the system performance exceeded our expectations.

17. Key Words (Suggested by Author(s))	18. Distribution Statement
Birefringent Sensor for High-Temperature Spectral-Analyzer Readout Dyanmic Birefringence Measurement Multichannel Stress Birefringence Readout	Unclassifed - Unlimited Subject Category 74

19. Security Classif. (of this report)	20. Security Classif. (of this page)	21. No. of pages	22. Price
Unclassified	Unclassified	61	A04

NASA FORM 1626 OCT 86